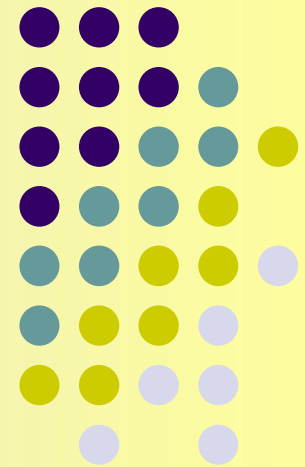


Exploring the possibility of studying the Drell-Yang process in the SPD (NICA) experiment.

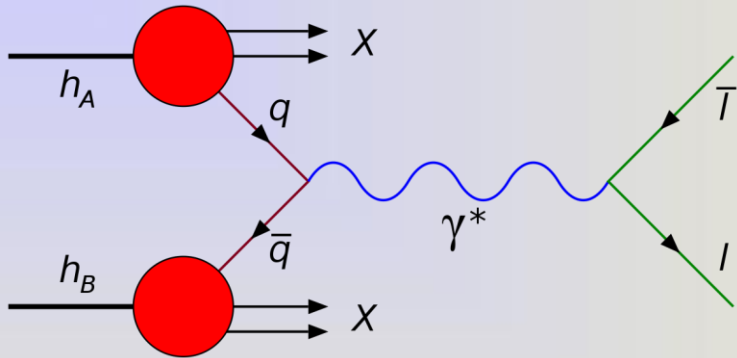


A.N.Skachkova
(JINR, Dubna)

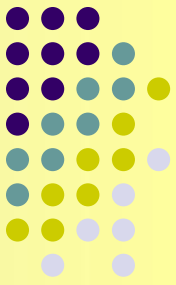
The XV-th International
School-Conference
"The Actual Problems of
Microworld Physics"



Minsk, Belarus, 27 August – 3 September, 2023



The Drell-Yan processes are collisions of hadrons at high energies, which give rise to a neutral gauge boson — a virtual photon or a weak Z^0 boson - during the interaction of a quark and an antiquark, which then decays into a pair of oppositely charged leptons

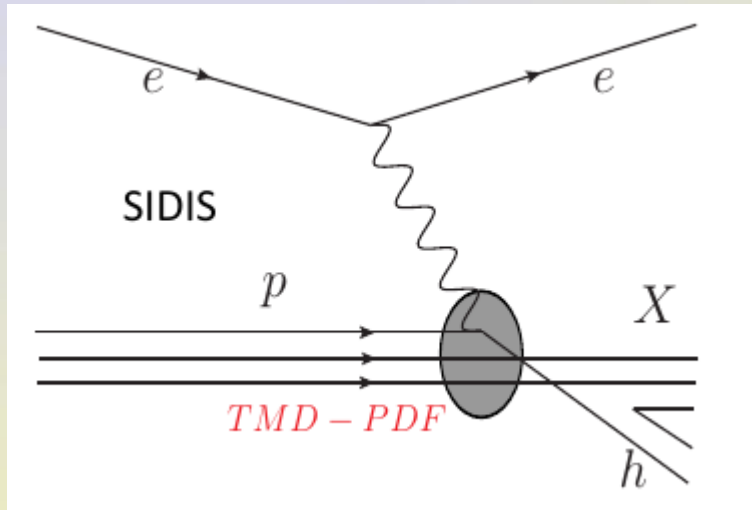
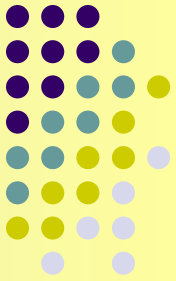


They are **unique processes for the study of spin effects** in hadron interactions, which **allow access to parton distributions** (*describing the distributions of quarks and gluons in hadrons (nuclei) by two variables: x (the fraction of the longitudinal momentum k of the hadron carried by the active parton) and p_T (the transverse momentum of the active parton)*) and **extract new information about the structure of nuclear matter and elementary particles.**

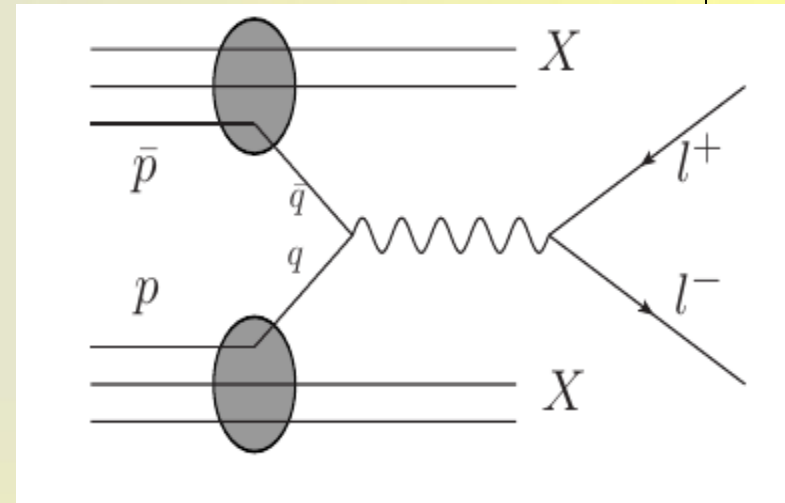
Precision extraction of parton distributions from some experimental data makes it possible to use them for predictions in other physical processes.

Experimental studies of the Drell-Yan processes make it possible to directly measure various spin asymmetries in collisions of unpolarized, transversely and longitudinally polarized hadrons.

Drell-Yang reactions are an important complement to other reactions (such as, for example, semi-inclusive deep-elastic scattering reactions (SIDIS)).

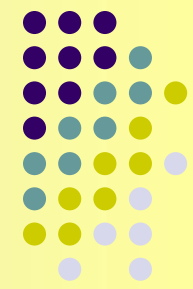


**TMD-PDF
related to fragmentation
functions**

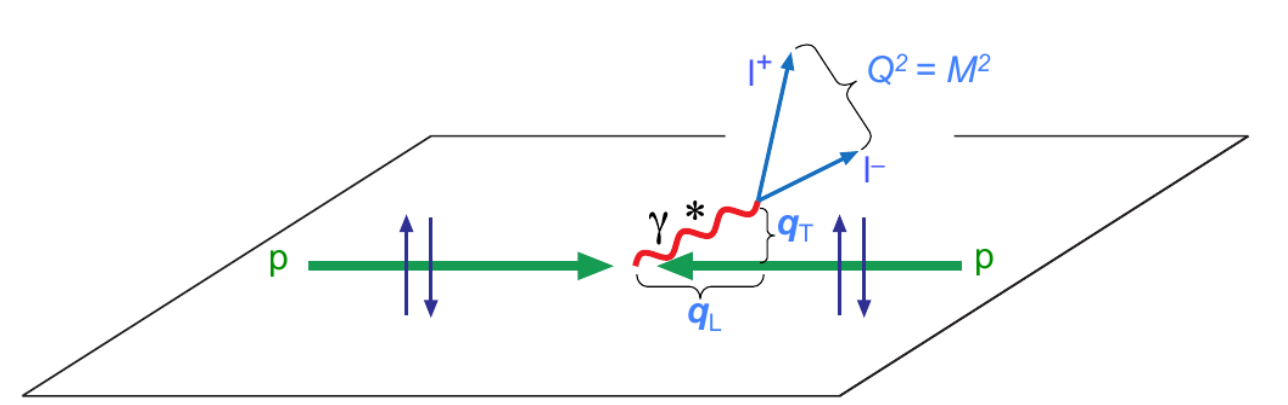


**Why Drell-Yan? –
Direct access to TMD-PDFs**

With respect to DIS (inclusive or semi-inclusive) by rotating the Feynman diagram, Drell-Yan is an s-channel process, and SIDIS is a t-channel process



The analysis of the measured spin characteristics allows us to extract information about the parton pulse distributions TMD (*relative to the transverse and longitudinal pulse of the active parton*) and PDF (*relative to the longitudinal pulse of the active parton*), **which are universal non-perturbative functions** (*describing effects at large distances / or at small pulse values*), **independent of the type of physical process characteristics** (*with the exception of T-odd TMD (T-odd TMD of Boer-Mulders and Sievers), changing the sign in the SIDIS and Drell-Yan processes*).

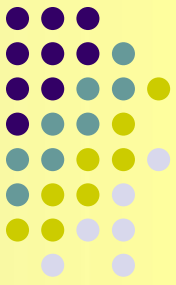


Partonic distributions are matrix elements of operators constructed in terms of quark and gluon fields and averaged over hadron states (vacuum states)

$$d\sigma^{D-Y} = \sum_{q, \bar{q}} f_q(x_1, \mathbf{k}_{\perp 1}; Q^2) \otimes f_{\bar{q}}(x_2, \mathbf{k}_{\perp 2}; Q^2) d\hat{\sigma}^{q\bar{q} \rightarrow \ell^+ \ell^-}$$

To extract **PDF distributions**, the most suitable conditions are when $M^{l+l-}_{inv} (=Q - \text{transmitted 4- momentum})$ and PT^{l+l-} are of the same order.
 To extract information about **TMD distributions**, the scale of $M^{l+l-}_{inv} (=Q) \gg PT^{l+l-}$ of lepton pair \sim transverse momentum of quarks and gluons k_T inside colliding hadrons is ideal.

Parton Distribution Functions



A number of PDFs depends on the order of the QCD approximations.

At leading order (LO, twist-2) 3 collinear (integrated over kt) PDFs are needed for a full description of the nucleon structure:

		nucleon polarisation		
		U	L	T
quark polarisation	U	f_1 number density q		
	L		g_1 helicity Δq	
	T			h_1 transversity

The PDFs f_1 and g_1 are measured rather well. The PDF $h_1(x, Q^2)$ is poorly studied. *It was historically introduced right for DY process.*

- Density $f_1(x, Q^2)$** — distribution of the parton Number/ probability to find quarks within the non-polarized (U) nucleon carrying a fraction x of the nucleon momentum

$$f_1 = \text{[diagram: circle with dot]}$$

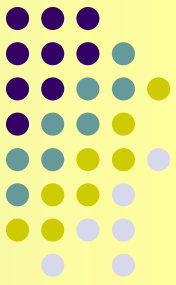
- Helicity (chirality) $g_1(x, Q^2) \equiv g_{1L}(x, Q^2)$** distribution of longitudinal polarization of quarks in longitudinally polarized (L) nucleon/ the difference in probabilities to find quarks in a longitudinally polarized nucleon with their spin aligned or anti-aligned to the spin of the nucleon

$$g_{1L} = \text{[diagram: circle with dot and arrow pointing right]} - \text{[diagram: circle with dot and arrow pointing left]}$$

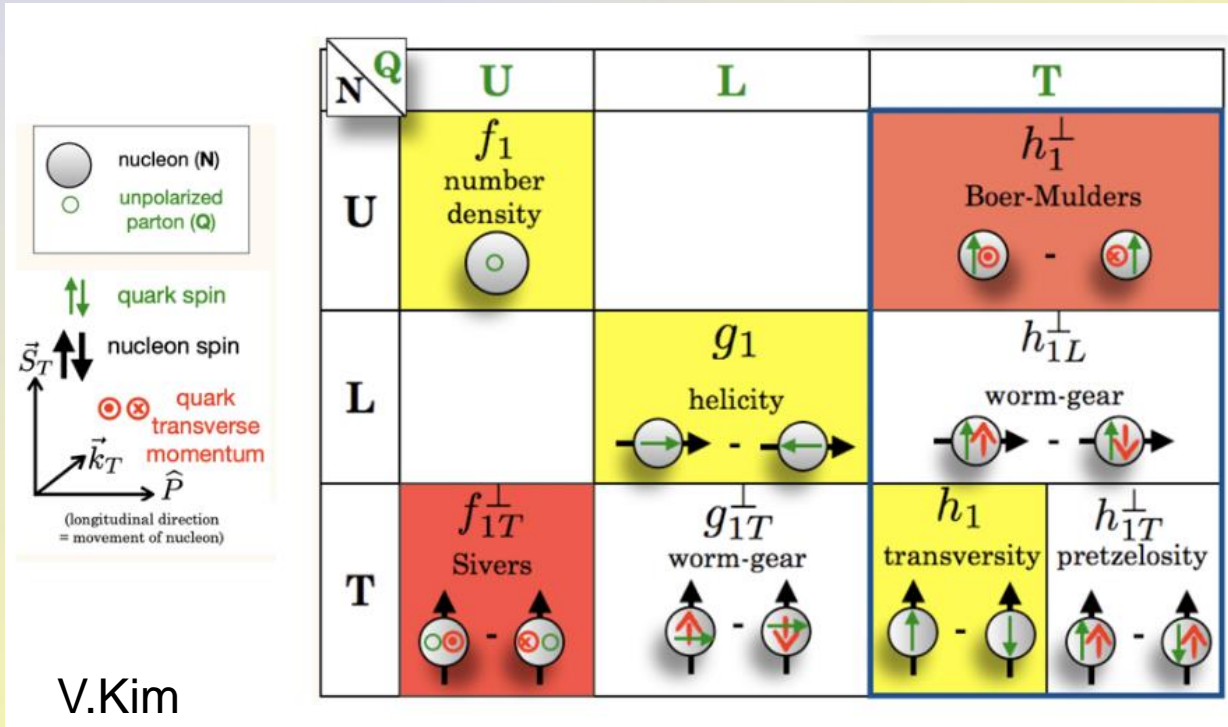
- Transversity $h_1(x, Q^2)$** - distribution of transverse polarization of quarks in transversely polarized (T) nucleon

$$h_{1T} = \text{[diagram: circle with dot and arrow pointing up]} - \text{[diagram: circle with dot and arrow pointing down]}$$

The structure of the proton: TMD PDF



Taking into account the **quark intrinsic transverse momentum k_T** , at leading order 8 TMD **(5 additional) PDFs** are needed for a full description of the nucleon structure, which are *functions of 3 variables* (x, k_T, Q^2). They are vanishes when integrating over k_T .

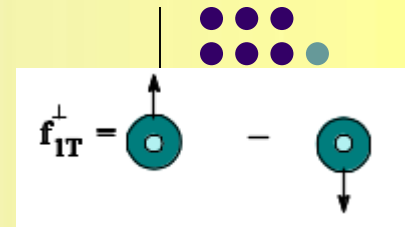


Leading twist TMD distribution functions. The **U, L, T** correspond to **unpolarized**, **longitudinally polarized** and **transversely polarized** nucleons (columns) and quarks (rows).

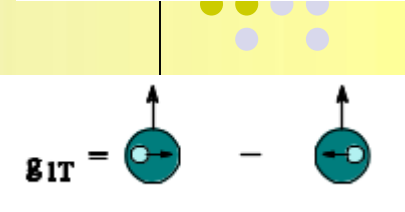
At the sub-leading twist (twist-3), there are still 16 TMD PDFs containing the information on the nucleon structure. *They have no definite physics interpretation yet.*

Since TMD distributions are nonperturbative functions, they **cannot be calculated within the framework of QCD**. Therefore, the main model-independent tool for studying TMD is **the analysis of spin effects in SIDIS and Drell-Yang processes**.

- f_{1T}^\perp (**Sivers**) - represents the distribution over the transverse momentum of non-polarized quarks in a transversely polarized nucleon (transverse spin);



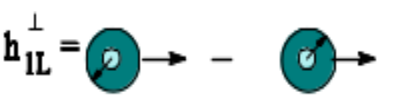
- g_{1T}^\perp (**Worm-gear-T**) - correlation between the transverse spin and the longitudinal quark polarization;



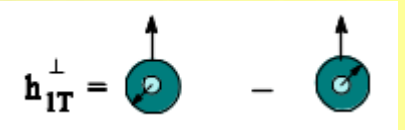
- h_1^\perp (**Boer-Mulders**) - distribution over the transverse momentum of transversely polarized quarks in the non-polarized nucleon ;



- h_{1L}^\perp (**Worm-gear-L**) - correlation between the longitudinal polarization of the nucleon (longitudinal spin) and the transverse momentum of quarks;



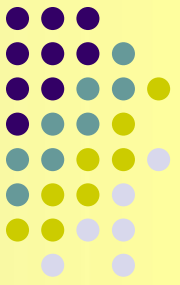
- h_{1T}^\perp (**Pretzelosity**) - distribution over the transverse momentum of transversely polarized quarks in the transversely polarized nucleon.



It is very **important to measure Worm-gear-T, L and Pretzelosity** which are still not measured or measured with large uncertainties.

The last one would give new information (at least within some models) on the **possible role of constituent`s orbital momenta in the resolution of the nucleon spin crisis.**

The PDFs studies via asymmetry of the DY pairs production cross sections

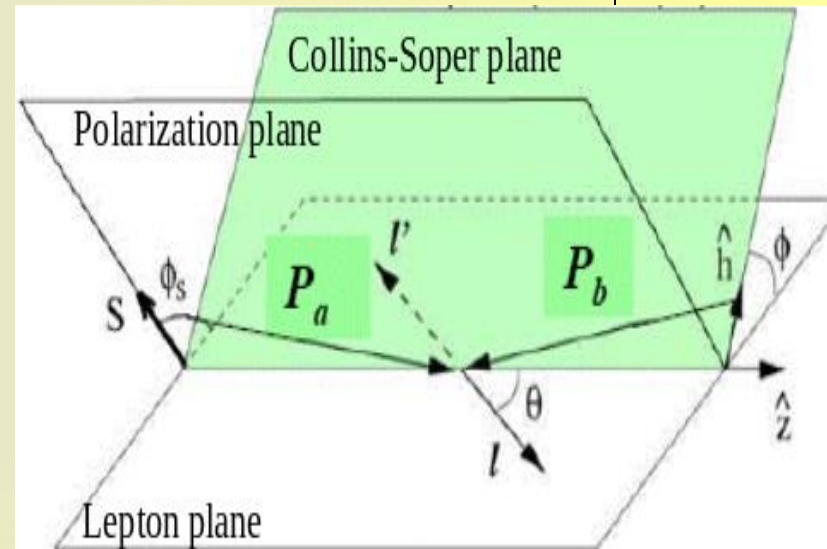


The **cross section** of the DY pair's production **cannot be measured directly** because there is **no single beam containing particles with the U, L and T polarization**.

To **measure SF's** one can use the following procedure:

1-st - to integrate differential cross section over the azimuthal **angle ϕ** between the Lepton and Hadron planes in the Collins-Soper reference frame,

2-nd - following the SIDIS practice, to measure azimuthal asymmetries of the DY pairs production cross sections.



The **azimuthal asymmetries** can be **calculated** as **ratios** of **cross sections differences** to the **sum** of the integrated over ϕ **cross sections σ_{int}** :

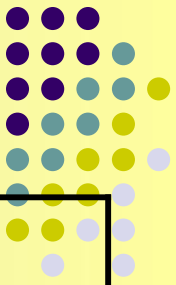
- The **numerator** of the ratio is calculated as a **difference** of the DY pair's production **cross sections** in the collision of hadrons h_a and h_b with **different polarizations**.
- The **denominator** of the ratio is calculated as a **sum of σ_{int} 's** calculated for the **same hadron polarizations** and same x_a, x_b regions **as in numerator**.

Previous Drell-Yan experiments



Experiment	Interaction	Reaction	Energy
CERN-NA3	pN(Pt)	p Nucleus \rightarrow μ^+ μ^- X	Plab = 400 GeV
CERN-NA10	π^- -N(W)	π^- Nucleus \rightarrow μ^+ μ^- X	Plab = 194, 286 GeV
CERN-NA58 (COMPASS)	π^- -p	π^- p \rightarrow μ^+ μ^- X	Plab = 190 GeV
CERN-WA11	π^- -N(Be)	π^- Nucleus \rightarrow μ^+ μ^- X	Plab = 150/175 GeV
CERN-WA39	π^+ -N(W) π^- -N(W)	π^+ Nucleus \rightarrow μ^+ μ^- X, π^- Nucleus \rightarrow μ^+ μ^- X	Plab = 39.5 GeV
CERN-R108	pp	p p \rightarrow e^+ e^- X	Plab(E_{cm}) = 62.4 GeV
CERN-R209	pp	p p \rightarrow μ^+ μ^- X	Plab (\sqrt{s}) = 44, 62 GeV
CERN-R808	pp	p p \rightarrow e^+ e^- X	Plab (\sqrt{s}) = 53, 63 GeV
CERN-UA2	\bar{p} p	\bar{p} p \rightarrow μ^+ μ^- X	Plab = 630 GeV
Fermilab-E288	pN(Pt)	p Nucleus \rightarrow μ^+ μ^- X	Plab = 200/300/400 GeV
Fermilab-E325	pN(Cu)	p Nucleus \rightarrow μ^+ μ^- X	Plab = 200,300,400 GeV
Fermilab-E326	π^- -N(W)	π^- Nucleus \rightarrow μ^+ μ^- X	Plab = 225 GeV
Fermilab-E439	pN(Cu)	p Nucleus \rightarrow μ^+ μ^- X	Plab = 400 GeV
Fermilab-E444	pN(C, Cu, W)	p Nucleus \rightarrow μ^+ μ^- X, π^+ Nucleus \rightarrow μ^+ μ^- X, π^- Nucleus \rightarrow μ^+ μ^- X	Plab = 225 GeV
Fermilab-E537	\bar{p} N(W), π^- -N(W)	\bar{p} p \rightarrow e^+ e^- X, \bar{p} N \rightarrow μ^+ μ^- X, π^- Nucleus \rightarrow μ^+ μ^- X	Plab = 125 GeV
Fermilab-E605	pN(Cu)	p Nucleus \rightarrow μ^+ μ^- X	Plab = 800 GeV
Fermilab-E615	π^- -N(W)	π^- Nucleus \rightarrow μ^+ μ^- X	Plab = 252 GeV
Fermilab-E740(D0)	\bar{p} p	\bar{p} p \rightarrow e^+ e^- X	E_{cms} (\sqrt{s}) = 1800 GeV
Fermilab-E741(CDF)	\bar{p} p	\bar{p} p \rightarrow μ^+ μ^- X , \bar{p} p \rightarrow e^+ e^- X	E_{cms} (\sqrt{s}) = 1800 GeV
Fermilab-E772	pp	p p \rightarrow μ^+ μ^- X	Plab = 800 GeV
Fermilab-E866(NUSEA)	pp	p p \rightarrow μ^+ μ^- X	Plab = 800 GeV

Experiments studying nucleon spin structure



<i>experiment</i>	CERN, COMPASS-II	FAIR, PANDA	FNAL, E-906	RHIC, STAR	RHIC- PHENIX	NICA, SPD
<i>mode</i>	Fixed Target	Fixed T.	Fixed T.	collider	collider	collider
<i>Beam/target</i>	π^-, p	anti-p, p	π^-, p	pp	pp	pp, pd, dd
<i>Polarization:b/t</i>	0; 0.8	0; 0	0; 0	0.5	0.5	0.9
<i>Luminosity</i>	$2 \cdot 10^{33}$	$2 \cdot 10^{32}$	$3.5 \cdot 10^{35}$	$5 \cdot 10^{32}$	$5 \cdot 10^{32}$	10^{32}
\sqrt{s} , GeV	19	<5.5	16	200, 500	200, 500	10 - 26
$x_{1(\text{beam})}$ range	0.1-0.9	0.1-0.8	0.1-0.5	0.03-1.0	0.03-1.0	0.1-0.8
q_T , GeV	0.5 -4.0	0.5 -1.5	0.5 -3.0	1.0 -10.0	1.0 -10.0	0.5 -6.0
<i>Lepton pairs,</i>	$\mu-\mu^+$	$\mu-\mu^+$	$\mu-\mu^+$	$\mu-\mu^+$	$\mu-\mu^+$	$\mu-\mu^+$, $e+e^-$
<i>Data taking</i>	2015	>2025	2013	>2016	>2016	>2020
<i>Transversity</i>	NO	NO (?)	NO	YES	YES	YES
<i>Boer-Mulders</i>	YES	YES	YES	YES	YES	YES
<i>Sivers</i>	YES	YES (?)	YES	YES	YES	YES
<i>Pretzelosity</i>	NO	NO	NO	NO	YES	YES
<i>Worm Gear</i>	NO	NO	NO	NO	NO	YES

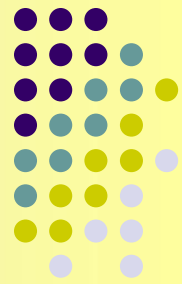


The tests at the SPD would have a number of advantages for DY measurements related to the nucleon structure studies:

- Running with **pp**, **pd** and **dd** beams,
- Scan of the effects over a *range of beam energies*,
- Running with **non-polarized**, **transverse** and **longitudinally polarized** beams and their combinations.

The above advantages would permit, for the first time, to perform comprehensive studies of **all leading twist PDFs** of the nucleon in a **single experiment** with minimal systematic errors.

SPD — Spin Physics Detector



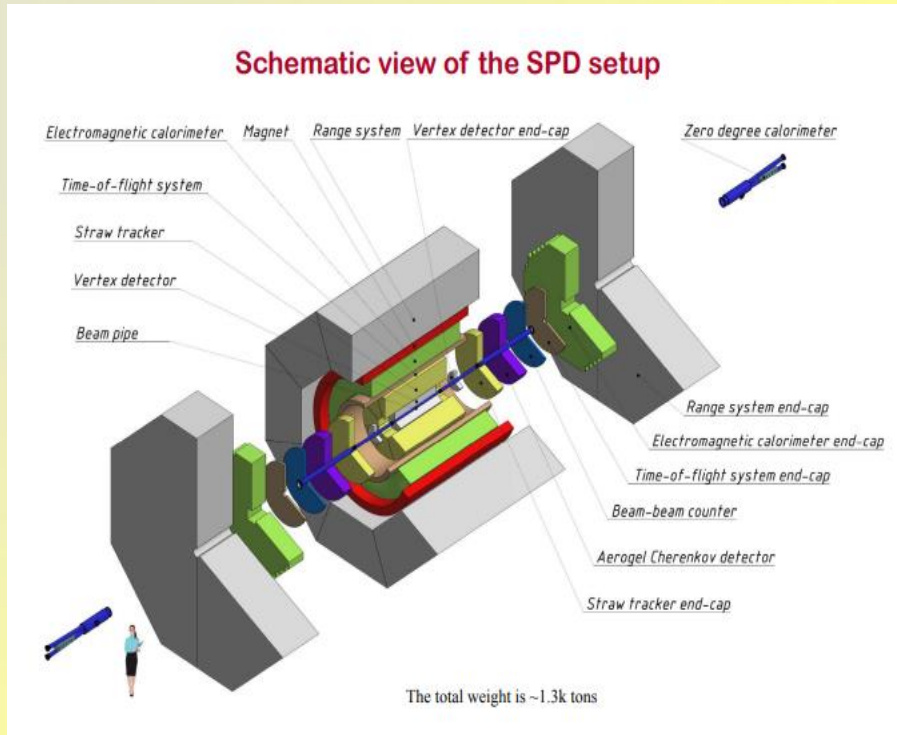
Beam energies:

$p\uparrow-p\uparrow(\sqrt{s_{pp}}) = 12 \div 27 \text{ GeV}$ (5 \div 12.6 GeV of proton kinetic energy),

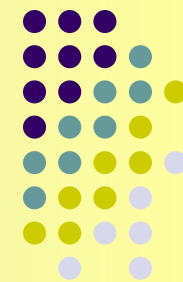
$d\uparrow-d\uparrow(\sqrt{s_{NN}}) = 4 \div 13.5 \text{ GeV}$ (2 \div 5.9 GeV/u of ion kinetic energy),

$p\uparrow-d\uparrow(\sqrt{s_{NN}}) \leq 19 \text{ GeV}$

- Luminosity up to $1 \cdot 10^{32} \text{ cm}^{-2}\text{s}^{-1}$ (p-p)
- $0.25 \cdot 10^{32} \text{ cm}^{-2}\text{s}^{-1}$ (d-d)
- Universal 4π detector with advanced tracking and particle identification capabilities based on modern technologies.
- Capability to detect events with high collision rate (up to 4MHz)
- Tracking : $\sim < 100 \mu\text{m}$ vertex resolution
- Photon detection with the energy resolution $\sim 5\%/E$
- Transverse momentum resolution $\sigma / p_T \approx 2\%$

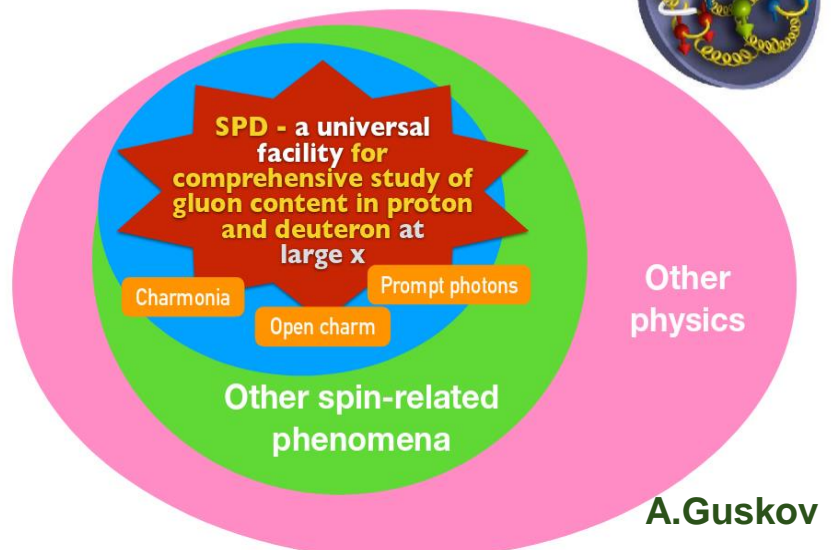


SPD Physics Program



The Spin Physics Detector (SPD) project aims to investigate the nucleon spin structure and polarization phenomena in polarized p - p and d - d collisions.

CONCEPT OF THE SPD PHYSICS PROGRAM



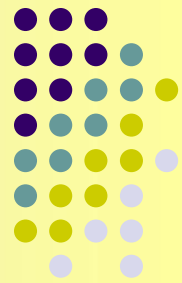
«Possible studies at the first stage of the NICA collider operation with polarized and unpolarized proton and deuteron beams» [arXiv:2102.08477](https://arxiv.org/abs/2102.08477), 2021

«On the physics potential to study the gluon content of proton and deuteron at NICA SPD» [arXiv:2011.15005](https://arxiv.org/abs/2011.15005), 2021

The plans to study Drell-Yan (DY) at SPD initially were the first in the list of physics proposal at SPD facility

«Spin Physics Experiments at NICA-SPD with polarized proton and deuteron beams».

Lol [arXiv:1408.3959](https://arxiv.org/abs/1408.3959), 2014



V.A. Matveev, R.M. Muradian, A.N. Tavkhelidze (MMT)

(V.A. Matveev, R.M. Muradian, A.N. Tavkhelidze, JINR-P2-4543, JINR, Dubna, 1969; SLAC-TRANS-0098)

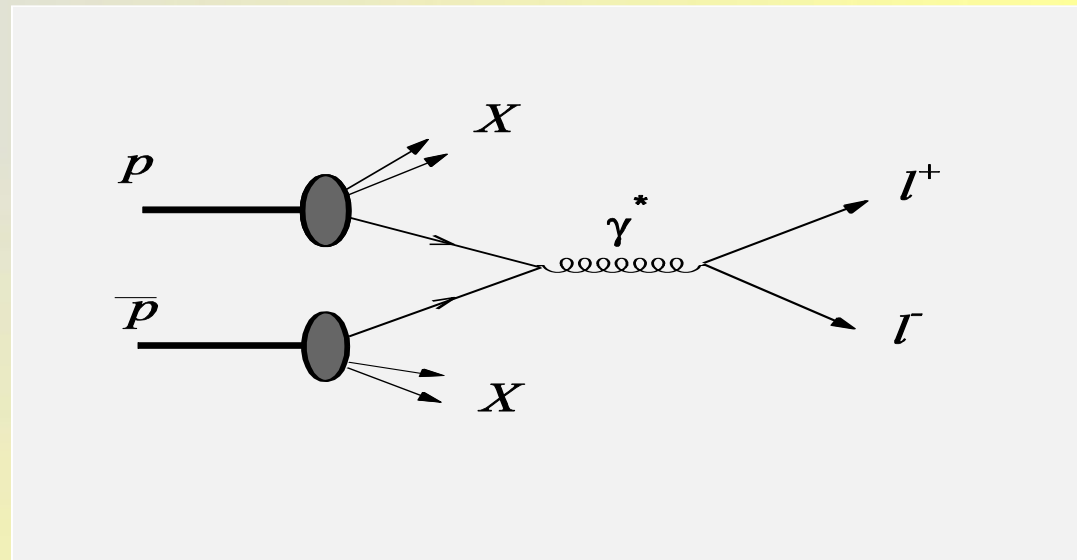
process, called also as Drell-Yan

(S.D. Drell, T.M. Yan, SLAC-PUB-0755, Jun 1970,12p.; Phys.Rev.Lett. 25(1970)316-320, 1970)

The dominant mechanism of the l^+l^- production is the perturbative QED/QCD partonic $2 \rightarrow 2$ process

$$\bar{q}q \rightarrow \gamma^* / Z^0 \rightarrow l^+l^-$$

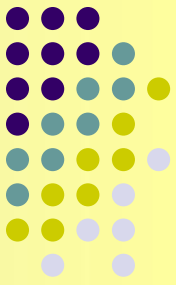
$$\sigma = 9.6 * 10^3 \text{ pb}$$



PYTHIA 6.4 simulation for the $E_{(p-p \text{ cms})} = 27 \text{ GeV}$

For the Luminosity $L = 1 \times 10^{32} \text{ cm}^{-2}\text{s}^{-1}$ with assumption of **10^7 sec/year** of beam operation we expect up to **$9.5 \times 10^6 \text{ Drell-Yan events/year}$** (without any cuts) & **$\sim 79\,700 \text{ Drell-Yan events/year}$** for $M_{\text{inv.}}(\mu^+\mu^-) > 4 \text{ GeV}$ (and first 2 cuts)

Main backgrounds



Main contribution to backgrounds for $\bar{q} q \rightarrow \gamma^* \rightarrow \mu^+ \mu^-$ process comes from two sources:

QCD (+charmonium) and Minimum-bias events

Initial conditions for simulation (both signal and BKG) are:
ISR, FSR, MPI – ON ; Lund fragmentation

We allow particles decay (and produce muons) in the volume before the Muon (Range) System :

cylindr radius $R = 2\,400\text{ mm}$ / size from the centre along Z axis $L = 4\,000\text{ mm}$
and search for muons in the angle region $3^\circ < \Theta < 177^\circ$

Contribution from b-quarks (subprocesses 81, 82, 461- 479) is negligible.

Total cross-section is $0.34 \times 10^{-6}\text{ mb}$. Initial $S/B \approx 27$.

Contribution from charmonia (subprocesses 86, 87-89, 104-105, 106, 421-439) **is less than from QCD and Mini-bias, but significant**.

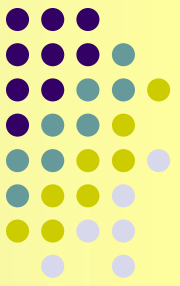
Their cross-section is $8.6 \times 10^{-4}\text{ mb}$. Initial $S/B = 1.0 \times 10^{-2}$.

Contribution from Charm production (subprocesses 81. $q + qbar \rightarrow c cbar$
82. $q + g \rightarrow c cbar$)

Total cross-section is $1.9 \times 10^{-3}\text{ mb}$. Initial $S/B \approx 5.2 \times 10^{-3}$

{Easy to suppress}

Main backgrounds



Now they are included in the **total list of QCD events** modeling
(subprocesses 10-14, 28-29, 53, 68)

The main contributions come from the following partonic subprocesses:

$q + q \rightarrow q + q$ (gives 43.5% of QCD events with the $\sigma = 92.7$ mb);

$g + g \rightarrow g + g$ (gives 46.7% of QCD events with the $\sigma = 99.5$ mb);

$q + q' \rightarrow q + q'$ (gives 9.2% of QCD events with the $\sigma = 19.7$ mb);

For QCD background $\sigma = 212.9$ mb, $S/B \approx 4.6 \times 10^{-8}$
(one order stronger than Mini-bias!)

Minimum-Bias processes

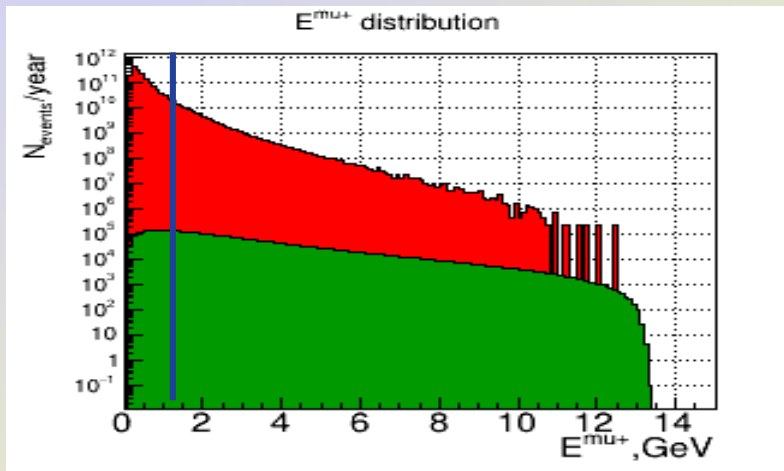
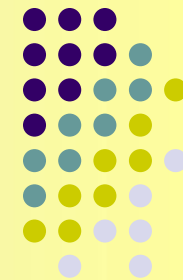
95. *Low - PT scattering* (~65% of MB events with the $\sigma = 14.0$ mb);

92-93. *Single diffractive* (24.8% of MB events with the $\sigma = 7.35$ mb);

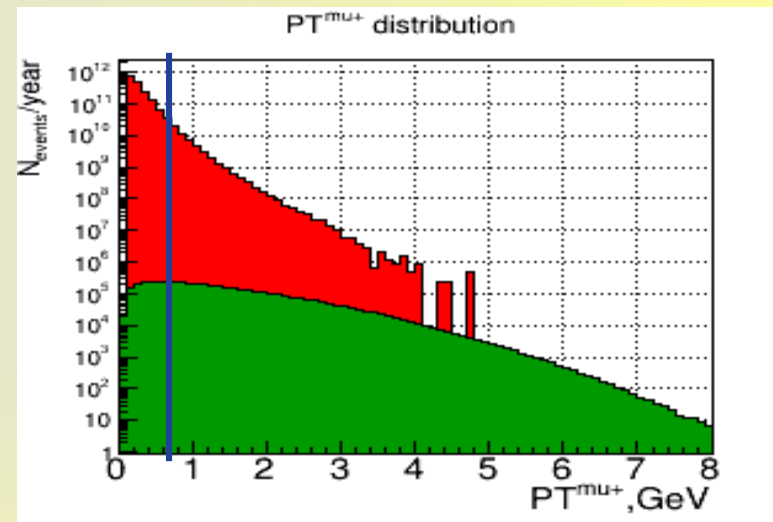
94. *Double diffractive* (7.2% of MB events with the $\sigma = 2.12$ mb);

$\sigma = 23.7$ mb. $S/B \approx 4.2 \times 10^{-7}$

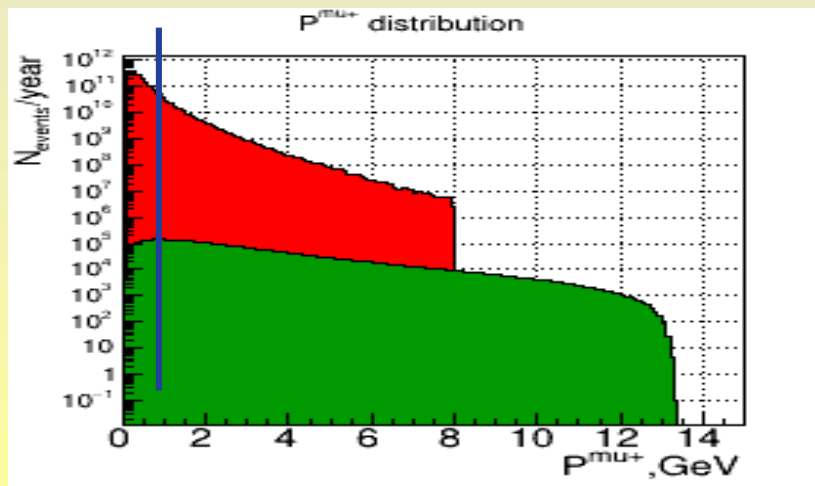
First cuts - on E(P) and PT



Effective cut off on E(P) only in the region
 $E^{\mu}_{bkg} < 1.5 \text{ GeV}$ (example $E^{\mu}_{bkg} = 1.0 \text{ GeV}$)
 where is the maximum gradient in E^{μ}_{bkg} distribution

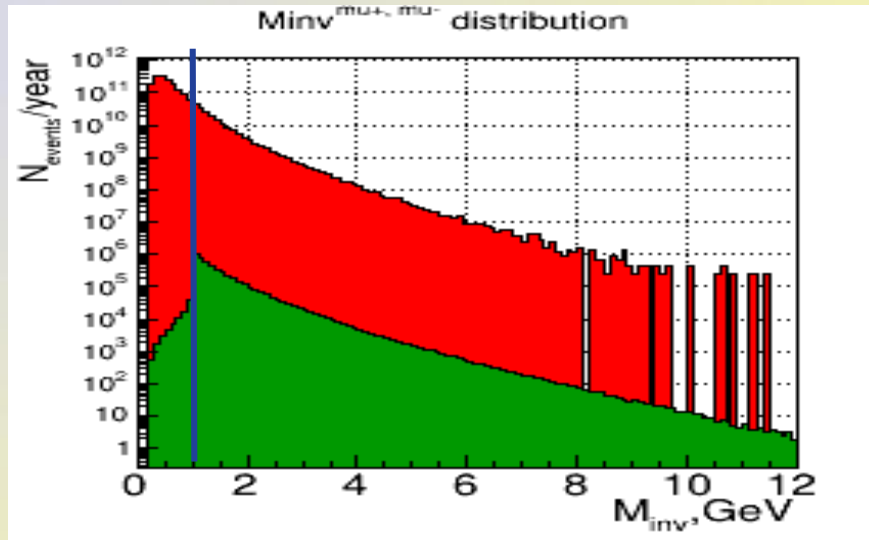
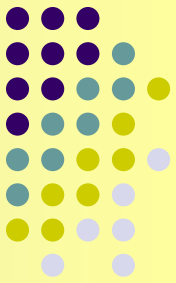


The most effective cuts off are in the region
 $PT^{\mu}_{bkg} < 1.5 \text{ GeV}$
 (for example $PT^{\mu}_{bkg} = 0.6 \text{ GeV}$)



Invariant mass cut

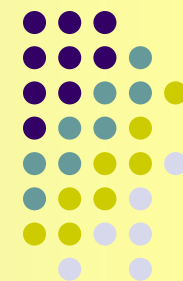
(picture corresponds to minimum-bias backgrounds)



The most effective cut is in the region **~ 1 GeV**.

Further increase of M_{inv} cut has no sense for Minimum-bias background events (it leads to significant loss of signal events without real improvement of S/B ratio) except backgrounds in the regions of J/Ψ and other resonances production.

Efficiency of $M_{inv} (\mu^+, \mu^-)$ cut



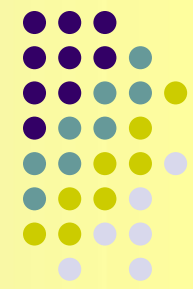
Together with the cut on $E(P)^\mu > 1 \text{ GeV}$, $PT^\mu > 0.6 \text{ GeV}$
and opposite sign leptons

$$\text{Cut efficiency} = \text{Nev}(\text{cutN}) / \text{Nev}(\text{init})$$

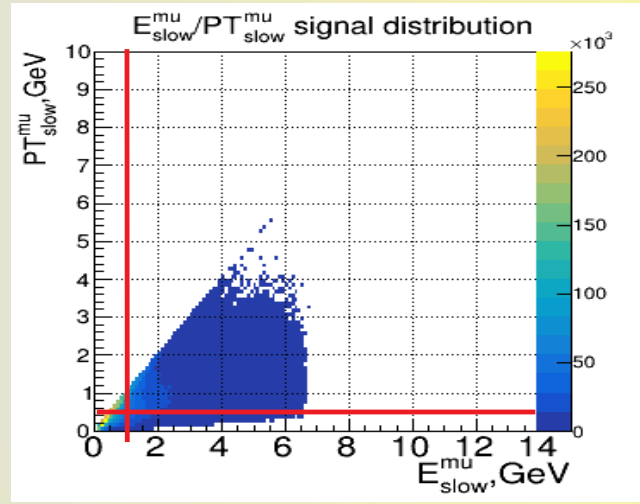
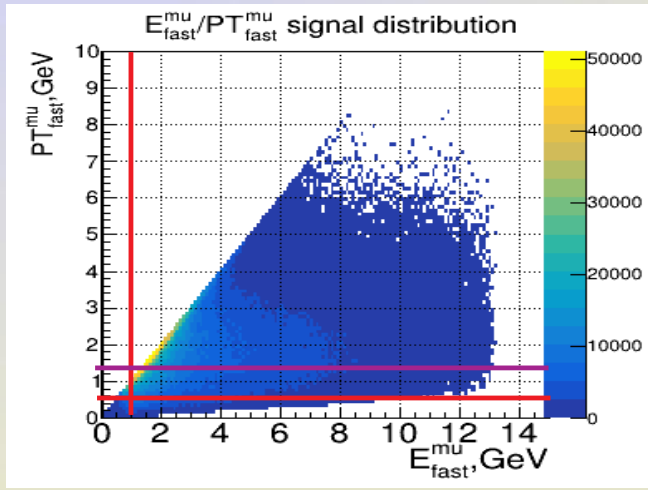
Minv cut	Rest of BKG	Cut efficiency for BKG	Rest of SIG	Rest of SIG events/year	Cut efficiency for SIG	S/B
$M_{inv}^{\mu\mu} > 1.0 \text{ GeV}$	$1.70 \times 10^{-2} \%$	1.36	40.5 %	3 869 571	1.02	$1.0 \times 10^{-4} \%$
$M_{inv}^{\mu\mu} > 1.5 \text{ GeV}$	$1.35 \times 10^{-2} \%$	1.69	16.7 %	1 595 601	2.97	$6.3 \times 10^{-5} \%$
$M_{inv}^{\mu\mu} > 2.0 \text{ GeV}$	$9.57 \times 10^{-3} \%$	2.41	8.3 %	793 023	7.28	$4.4 \times 10^{-5} \%$
$M_{inv}^{\mu\mu} > 2.5 \text{ GeV}$	$6.05 \times 10^{-3} \%$	3.80	4.5 %	429 952	15.9	$3.8 \times 10^{-5} \%$
$M_{inv}^{\mu\mu} > 3.0 \text{ GeV}$	$3.70 \times 10^{-3} \%$	6.22	2.5 %	238 862	32.0	$3.4 \times 10^{-5} \%$
$M_{inv}^{\mu\mu} > 3.5 \text{ GeV}$	$2.24 \times 10^{-3} \%$	10.3	1.4 %	133 762	60.7	$3.2 \times 10^{-5} \%$
$M_{inv}^{\mu\mu} > 4.0 \text{ GeV}$	$1.38 \times 10^{-3} \%$	16.7	0.8 %	76 435	110.1	$2.9 \times 10^{-5} \%$
$M_{inv}^{\mu\mu} > 4.5 \text{ GeV}$	$8.49 \times 10^{-4} \%$	27.1	0.5 %	47 772	192.2	$3.0 \times 10^{-5} \%$
$M_{inv}^{\mu\mu} > 5.0 \text{ GeV}$	$5.28 \times 10^{-4} \%$	43.7	0.3 %	28 663	328.0	$2.9 \times 10^{-5} \%$

Minv cut doesn't influence much on S/B ratio. But at **$M_{inv}^{\mu\mu} > 4.0 \text{ GeV}$** we have **too small number of events/year.**

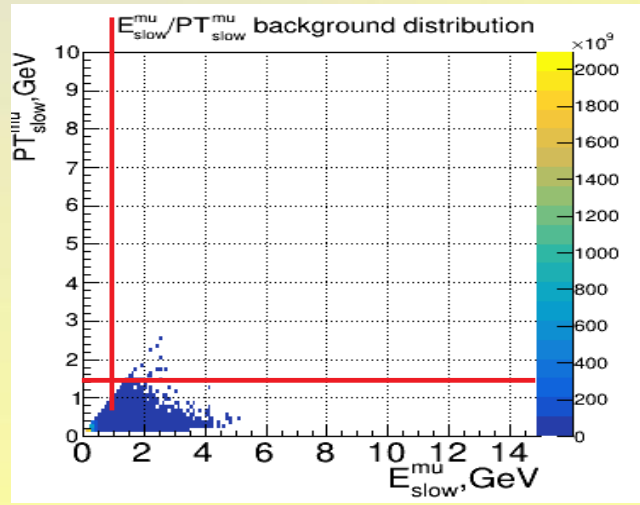
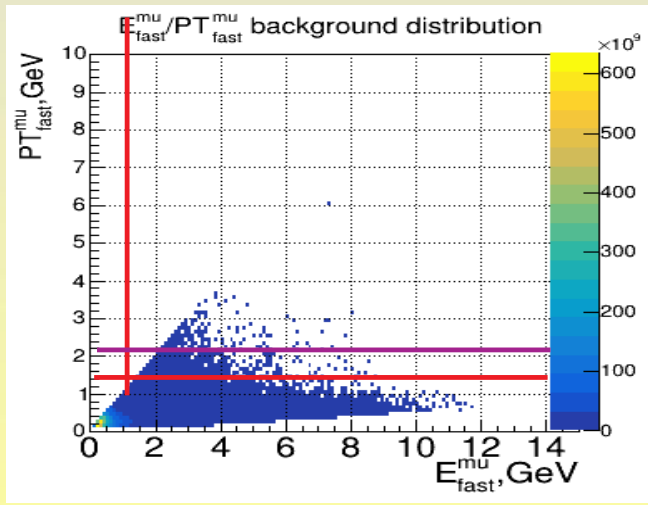
E^μ/PT^μ correlations for muons with max(fast) / min(slow) E^μ in the pair



S
I
G



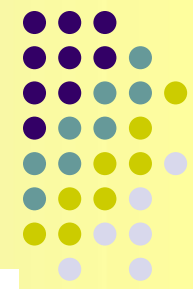
B
K
G



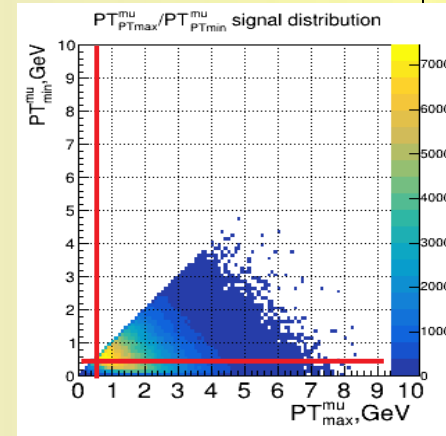
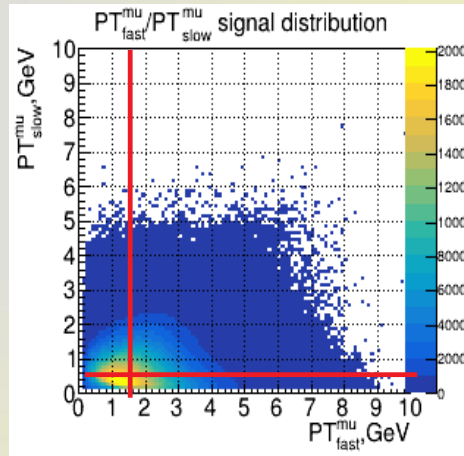
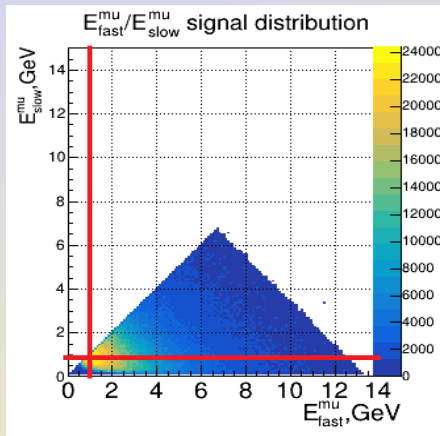
$PT^\mu_{fast} > 1.5 \text{ GeV}$

Cut on $PT^\mu > 0.6 \text{ GeV}$ and $E^\mu > 1.0 \text{ GeV}$

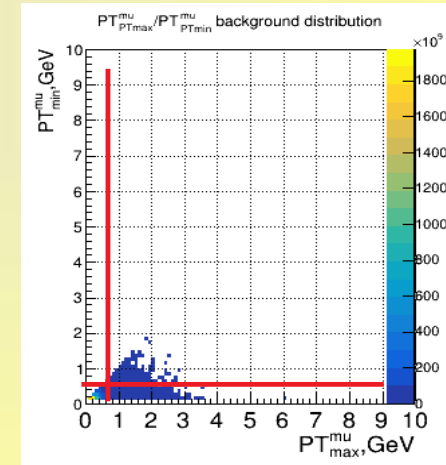
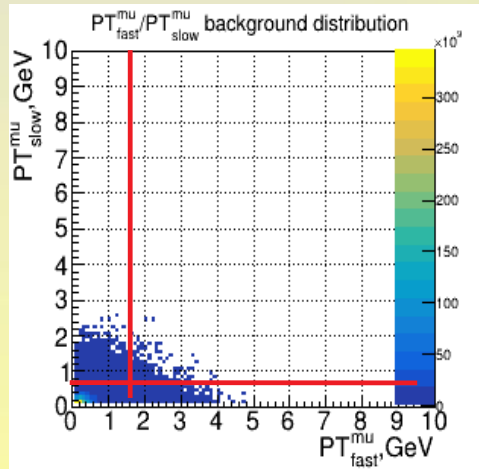
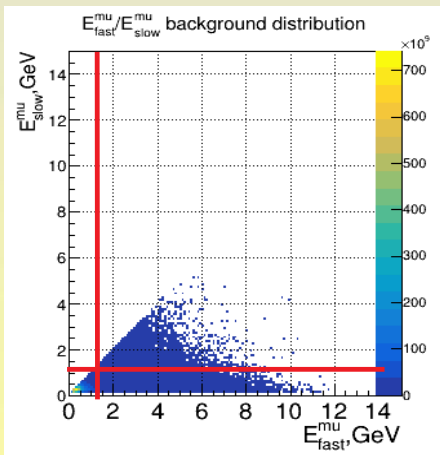
$E_{\text{fast}}^{\mu} / E_{\text{slow}}^{\mu}$, $PT_{\text{fast}}^{\mu} / PT_{\text{slow}}^{\mu}$, $PT_{\text{max}}^{\mu} / PT_{\text{min}}^{\mu}$ distributions



S
I
G



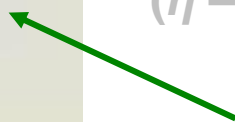
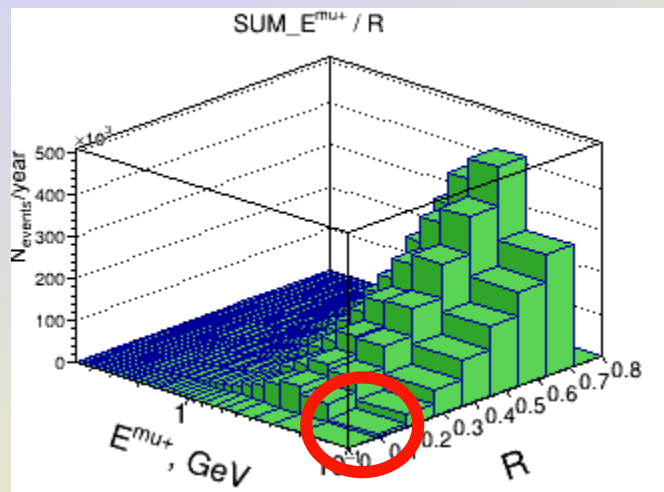
B
K
G



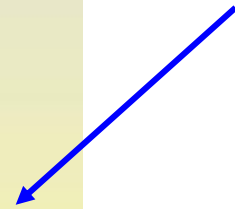
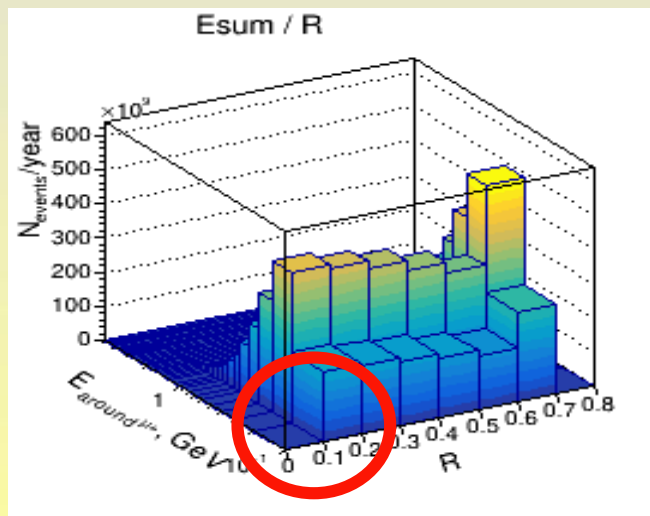
$E_{\text{fast}}^{\mu} > 1.0 \text{ GeV}$

$PT_{\text{fast}}^{\mu} > 1.5 \text{ GeV}$

$PT^{\mu} > 0.6 \text{ GeV}$



upper plot **signal events**

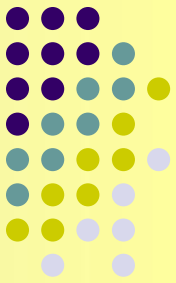


bottom plot **Mini-bias background**

Isolation criteria ($R_{\text{isolation}} = 0.2$)
 E_{sum} (of particles) < 0.5 GeV

allows to separate most part of Mini-bias & QCD bkg muons
 with additional loss of **0.7%** of signal events
after applied cuts discussed above

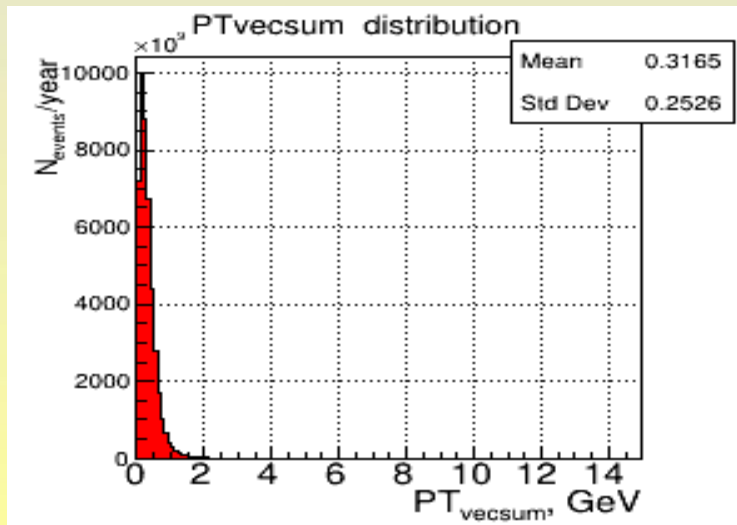
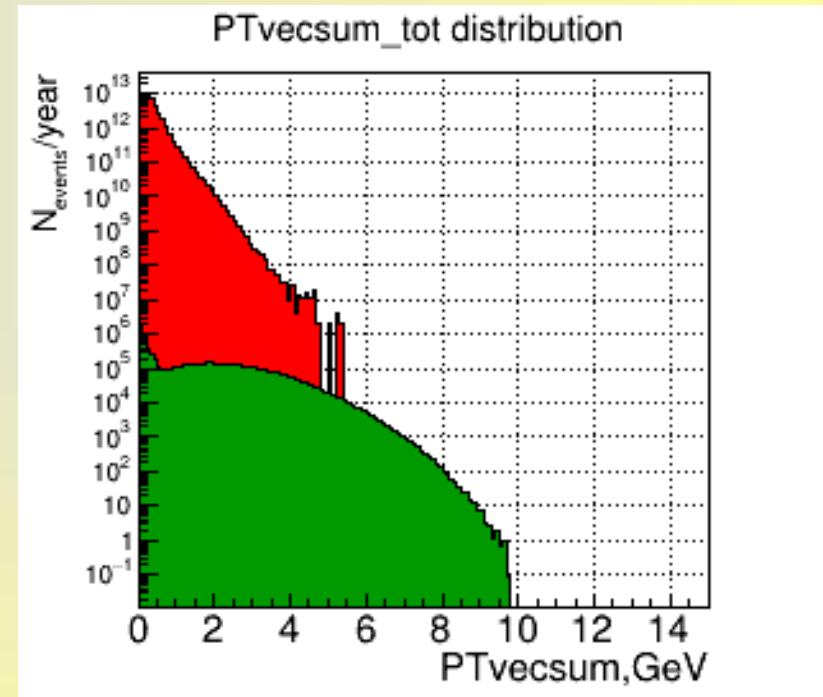
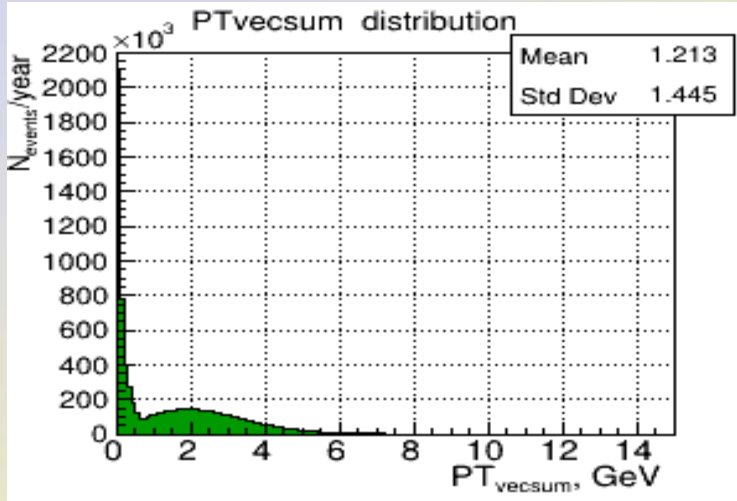
Cut on PT_{vecsum} - vector sum of all particles transverse momenta in event



S
I
G

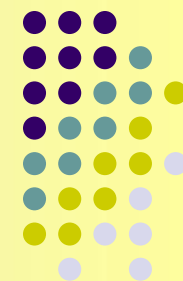
B
K
G

Sig & BKG
in log scale



$PT_{vecsum} < 0.2 \text{ GeV}$
BKG suppression factor (Eff) = 4

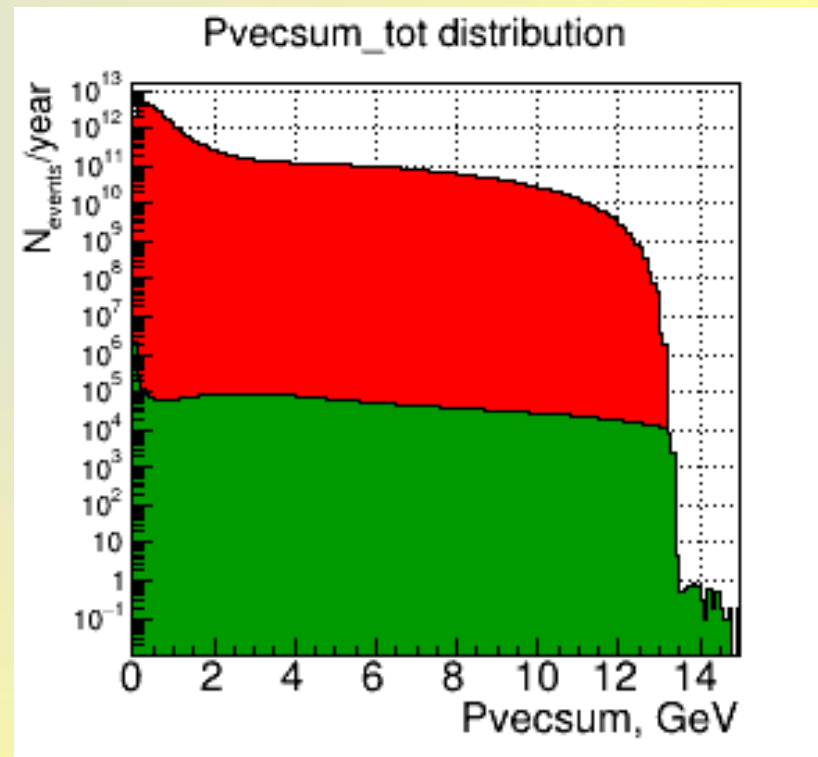
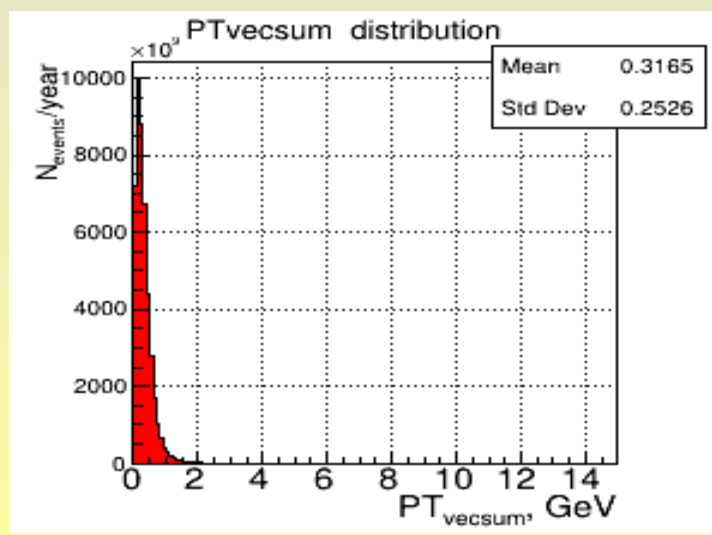
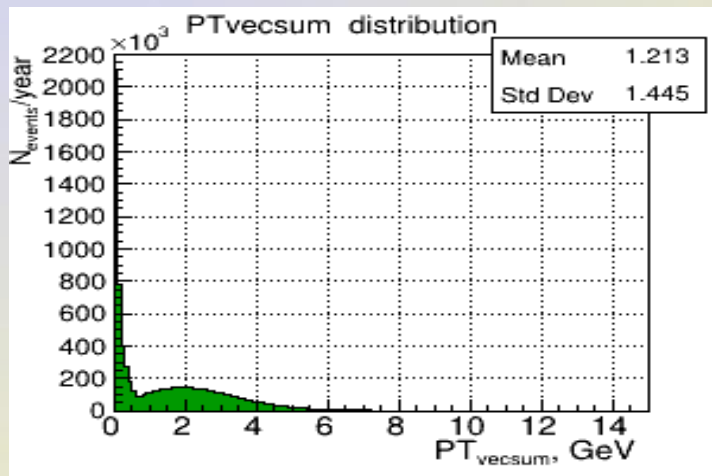
Analogous cut on P_{vecsum} - vector sum of all particles momenta in event



S
I
G

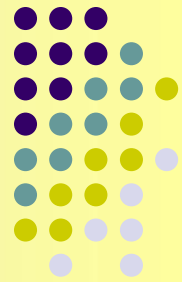
B
K
G

Sig & BKG
in log scale



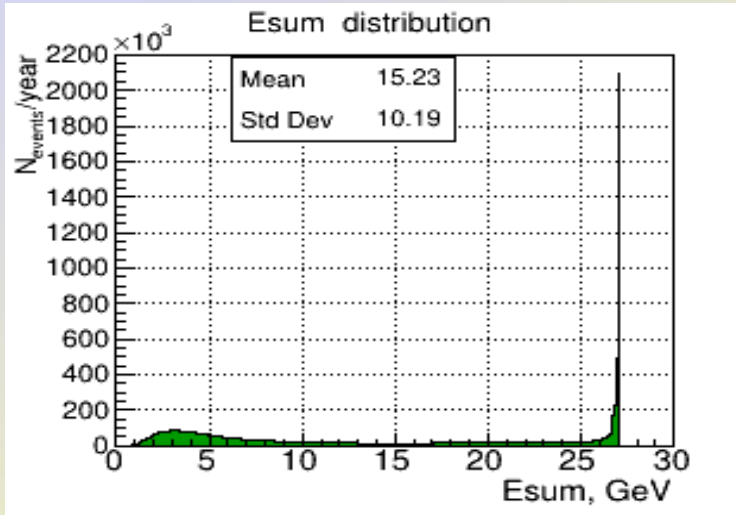
$P_{\text{vecsum}} < 0.2 \text{ GeV}$
BKG suppression factor (Eff) = 18 - 19

Cut on E_{sum} - summarized energy of all detected particles in event

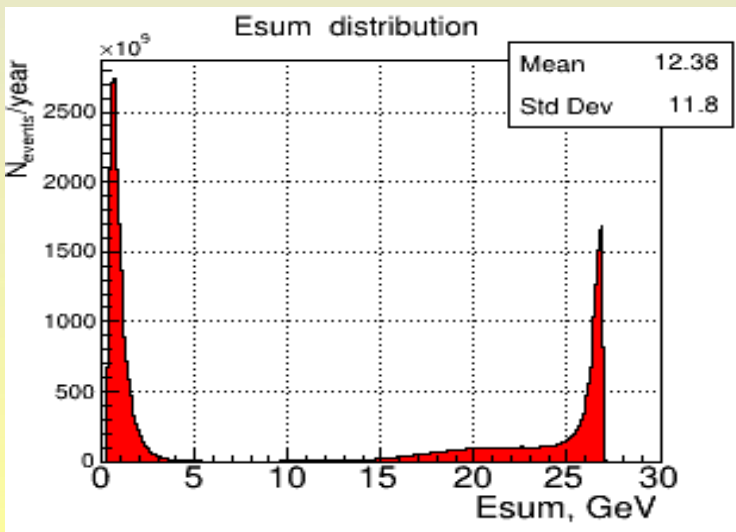
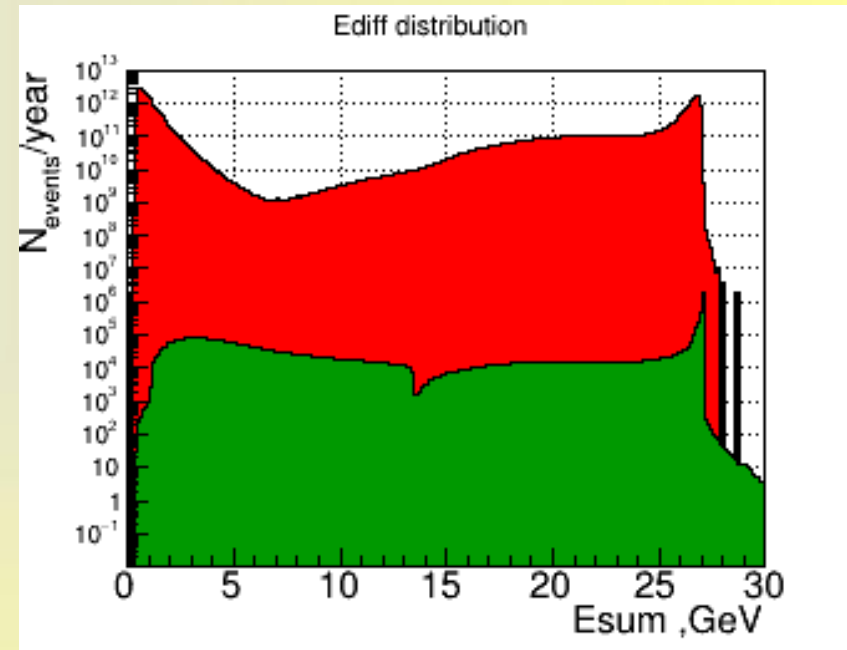


S
I
G

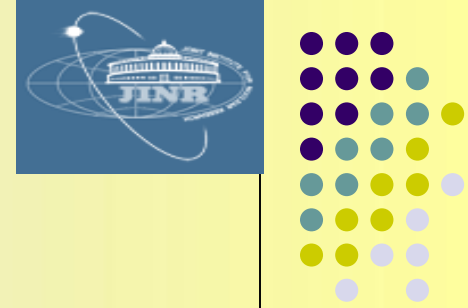
B
K
G



Sig & BKG
in log scale



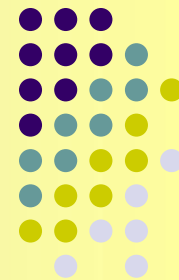
$E_{\text{sum}} > 26.8 \text{ GeV}$
BKG suppression factor (Eff) =
58 (MB) – 67 (QCD)



1. Events with only **2** muons with $PT^\mu > 0.6 \text{ GeV}$, $E^\mu > 1.0 \text{ GeV}$
2. Muons are of the **opposite sign**
3. $M_{\text{inv}}(\mu^+, \mu^-) > 1.0 \text{ GeV}$
4. $PT^\mu_{\text{fast}} > 1.5 \text{ GeV}$
5. The vertex of production placed within the **distance** from the interaction point $R < 1(30) \text{ mm}$
But! Fit program can misidentify μ and π as one track due to small angle of $\pi \rightarrow \mu (+\nu)$ decay .
6. Cut on summarized energy of all detected (without pipe zone and neutrino) particles in event $E_{\text{sum}} > 26.8 \text{ GeV}$
7. Isolation criterion $E_{\text{sum}}^{\text{sum}}(R \text{ isolation} = 0.2) < 0.5 \text{ GeV}$

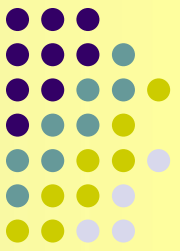
Cuts separate and summarized efficiency for Minimum-bias background events (10^9)

$$\text{Efficiency } \text{Eff}(K,N) = \text{Nev}(\text{cut}N) / \text{Nev}(\text{cut}K)$$



N of cuts	S/B ratio	Efficiency for BKG	Rest of BKG	Efficiency for SIG	Rest of SIG
1 Exactly 2μ with $PT^\mu > 0.6$ GeV, $P(E)^\mu > 1.0$ GeV	$5.1 * 10^{-4}$	Eff (1,init) = 3480	$2.9 \times 10^{-2} \%$	2.3	44.1 %
2 ⁺¹ 2μ are of the opposite sign	$8.9 * 10^{-4}$	Eff (2,1) = 1.8	$1.6 \times 10^{-2} \%$	1.01	43.8 %
3 ⁺²⁺¹ $M_{inv}(\mu^+, \mu^-) > 1.0$ GeV	$1.2 * 10^{-3}$	Eff (3,2) = 1.3	$1.2 \times 10^{-2} \%$	1.01	43.8 %
4 ⁺³⁺²⁺¹ $PT^\mu_{Emax} > 1.5$ GeV	$1.1 * 10^{-2}$	Eff (4,3) = 13.2	$9.1 \times 10^{-4} \%$	1.43	30.5 %
5 ⁺³⁺²⁺¹ $E_{sum}^{all} > 26.8$ GeV	$2.6 * 10^{-2}$	Eff (5,3) = 58.3	$2.1 \times 10^{-4} \%$	2.63	16.6 %
6 ⁺³⁺²⁺¹ $PT_{vecsum}^{all} < 0.2$ GeV	$2.9 * 10^{-3}$	Eff (6,3) = 4.1	$2.9 \times 10^{-3} \%$	1.70	25.7 %
7 ⁺³⁺²⁺¹ $p_{vecsum}^{all} < 0.2$ GeV	$9.4 * 10^{-3}$	Eff (7,3) = 18.4	$6.5 \times 10^{-4} \%$	2.34	18.7 %
8 ⁺³⁺²⁺¹ Isolation criterium	47.6	Eff (8,3) = 30177	$4.0 \times 10^{-7} \%$	1.01	43.2 %
9 ⁺³⁺²⁺¹ $R_{vertex} < 1$ mm	$8.5 * 10^{-1}$	Eff (9,3) = 710	$1.7 \times 10^{-5} \%$	1.01	43.5 %
10 ⁺³⁺²⁺¹ $R_{vertex} < 30$ mm	$7.1 * 10^{-1}$	Eff (10,3) = 597	$2.0 \times 10^{-5} \%$	1.01	43.5 %
5 ⁺⁴⁺³⁺²⁺¹ $E_{sum}^{all} > 26.8$ GeV	$2.3 * 10^{-1}$	Eff (5,4) = 52.7	$1.7 \times 10^{-5} \%$	2.52	12.1 %
8 ⁺⁴⁺³⁺²⁺¹ Isolation criterium	24.7	Eff (8,4) = 2280	$4.0 \times 10^{-7} \%$	1.02	29.9 %
8 ⁺⁵⁺⁴⁺³⁺²⁺¹ Isolation criterium	> 54	Eff (8,5) > 173	$< 1.0 \times 10^{-7} \%$	1.87	16.3 %

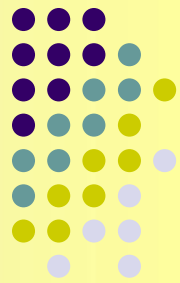
Cuts separate and summarized efficiency for QCD (+charmonia) background events (10^9)



$$\text{Efficiency } \text{Eff}(K,N) = \text{Nev}(\text{cut}N) / \text{Nev}(\text{cut}K)$$

N of cuts	S/B ratio	Efficiency for BKG	Rest of BKG	Efficiency for SIG	Rest of SIG
1 Exactly 2μ with $\text{PT}^\mu > 0.6$ GeV, $\text{P}(E)^\mu > 1.0$ GeV	$4.4 * 10^{-5}$	Eff (1,init) = 2471	$4.0 \times 10^{-2} \%$	2.8	35.3 %
2 ⁺¹ 2μ are of the opposite sign	$7.4 * 10^{-5}$	Eff (2,1) = 1.7	$2.3 \times 10^{-2} \%$	1.2	33.3 %
3 ⁺²⁺¹ $M_{\text{inv}}(\mu^+, \mu^-) > 1.0$ GeV	$1.0 * 10^{-4}$	Eff (3,2) = 1.3	$1.7 \times 10^{-2} \%$	1.0	33.3 %
4 ⁺³⁺²⁺¹ $\text{PT}^\mu_{\text{Emax}} > 1.5$ GeV	$7.4 * 10^{-4}$	Eff (4,3) = 14.1	$1.2 \times 10^{-3} \%$	1.9	17.6 %
5 ⁺³⁺²⁺¹ $E^{\text{all}}_{\text{sum}} > 26.8$ GeV	$2.4 * 10^{-3}$	Eff (5,3) = 67.4	$2.5 \times 10^{-4} \%$	2.8	11.7%
6 ⁺³⁺²⁺¹ $\text{PT}^{\text{all}}_{\text{vecsum}} < 0.2$ GeV	$2.5 * 10^{-4}$	Eff (6,3) = 4.2	$4.0 \times 10^{-3} \%$	1.7	19.6 %
7 ⁺³⁺²⁺¹ $\text{P}^{\text{all}}_{\text{vecsum}} < 0.2$ GeV	$9.3 * 10^{-4}$	Eff (7,3) = 19.7	$8.6 \times 10^{-4} \%$	2.2	15.7 %
8 ⁺³⁺²⁺¹ Isolation criterium	> 17	Eff (8,3) > 169847	$< 1.0 \times 10^{-7} \%$	1.0	33.3 %
9 ⁺³⁺²⁺¹ $R_{\text{vertex}} < 1$ mm	$5.5 * 10^{-2}$	Eff (9,3) = 551	$3.0 \times 10^{-5} \%$	1.0	33.3 %
10 ⁺³⁺²⁺¹ $R_{\text{vertex}} < 30$ mm	$4.8 * 10^{-2}$	Eff (10,3) = 479	$3.5 \times 10^{-5} \%$	1.0	33.3 %
5 ⁺⁴⁺³⁺²⁺¹ $E^{\text{all}}_{\text{sum}} > 26.8$ GeV	$1.6 * 10^{-2}$	Eff (5,4) = 64.5	$1.8 \times 10^{-5} \%$	3.0	5.9 %
8 ⁺⁴⁺³⁺²⁺¹ Isolation criterium	> 9	Eff (8,4) > 12066	$< 1.0 \times 10^{-7} \%$	1.0	17.6 %
8 ⁺⁵⁺⁴⁺³⁺²⁺¹ Isolation criterium	> 3	Eff (8,5) > 187	$< 1.0 \times 10^{-7} \%$	1.0	5.9 %

Conclusion



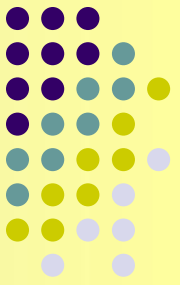
The proposed cuts:

1. Events with only **2** muons with $PT^\mu > 0.6 \text{ GeV}$, $E^\mu > 1.0 \text{ GeV}$
2. Muons are of the **opposite sign**
3. $M_{inv}(\mu^+, \mu^-) > 1.0 \text{ GeV}$
4. $PT^\mu_{fast} > 1.5 \text{ GeV}$
5. Cut on summarized energy of all detected (without pipe zone and neutrino) particles in event $E_{sum} > 26.8 \text{ GeV}$
6. Isolation criterion $E^{sum}_{(R \text{ isolation} = 0.2)} < 0.5 \text{ GeV}$

*Allow (in the ideal case) to suppress Mini-bias bkgd up to $S/B \sim 50$,
QCD background – up to $S/B > \sim 17$.*

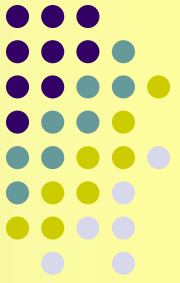
The SPD Collaboration made a decision to suspend the study of such reactions.

In fact, taking into account the detector and additional contributions of muon misidentification,
it will be difficult to experimentally isolate the DY signal from the combinatorial background.

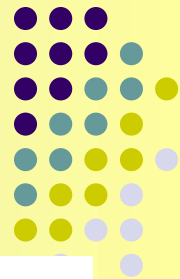


Thank you for your attention!

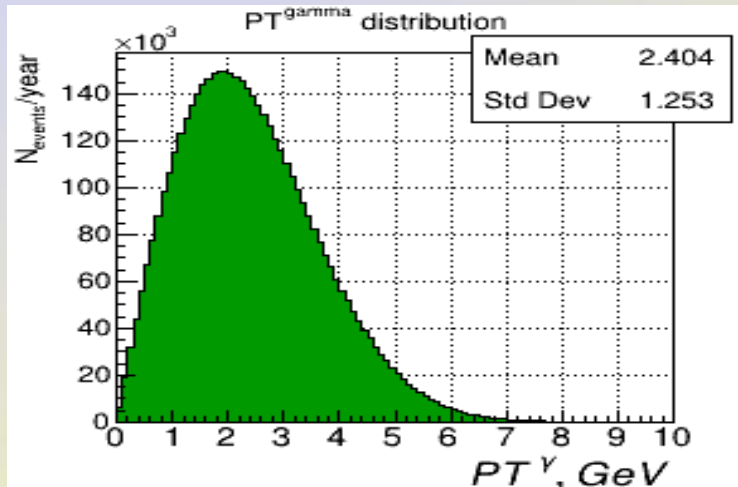
Back up slides



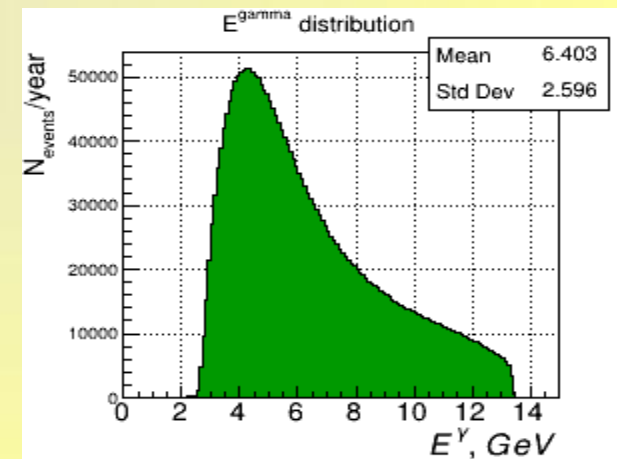
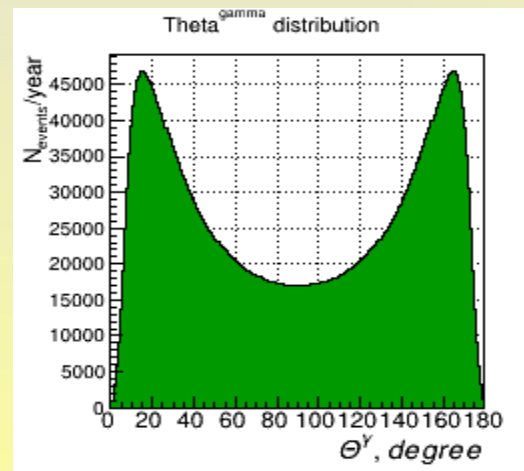
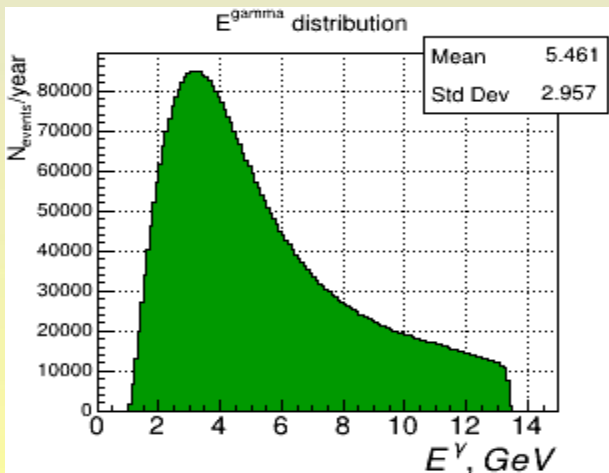
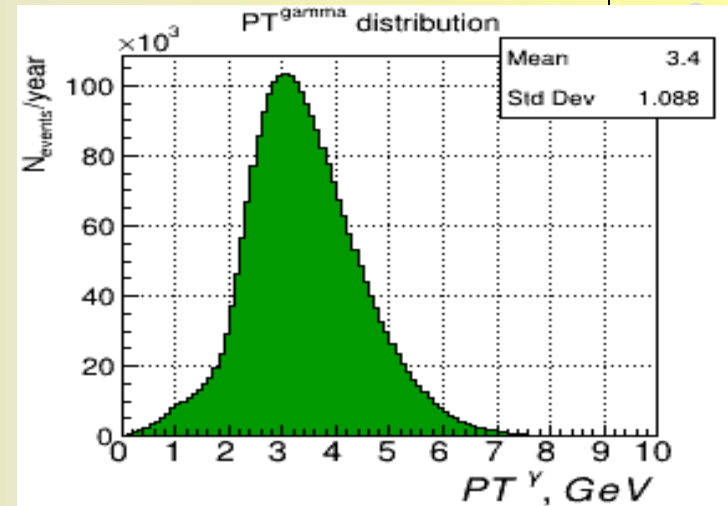
Intermediate γ^* distributions



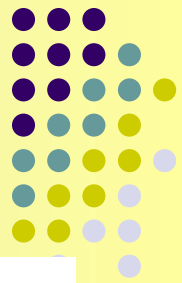
Without cuts



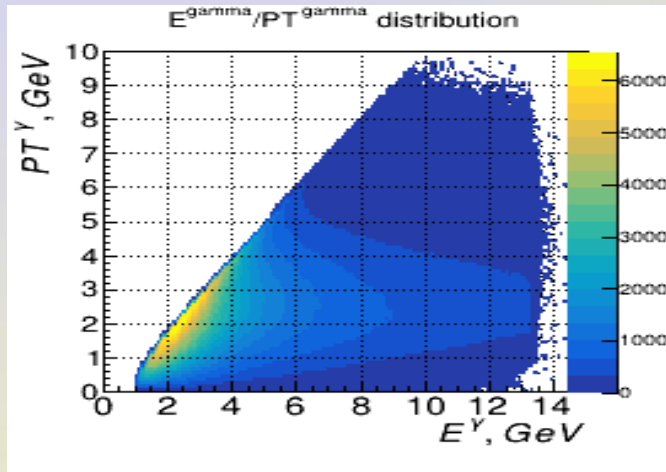
After cuts



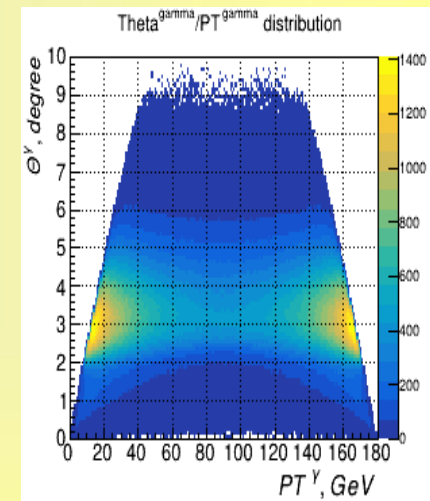
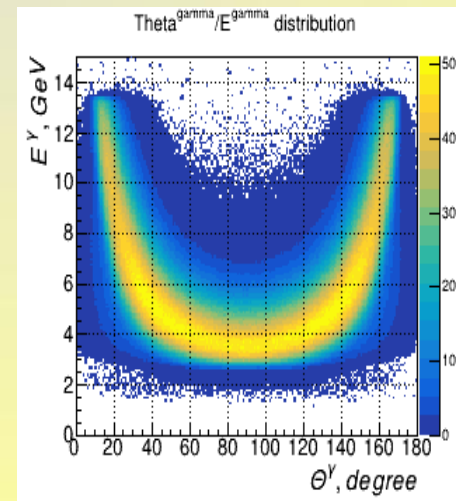
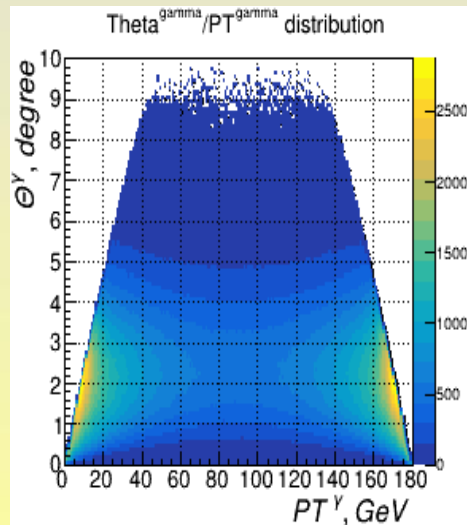
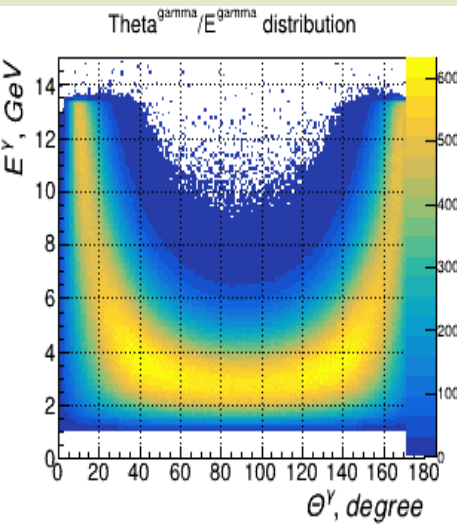
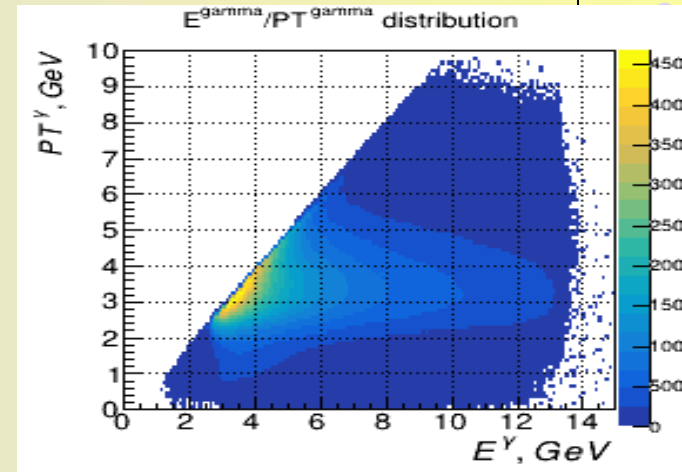
Intermediate γ^* correlation distributions



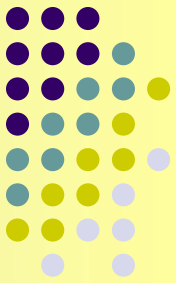
Without cuts



After cuts



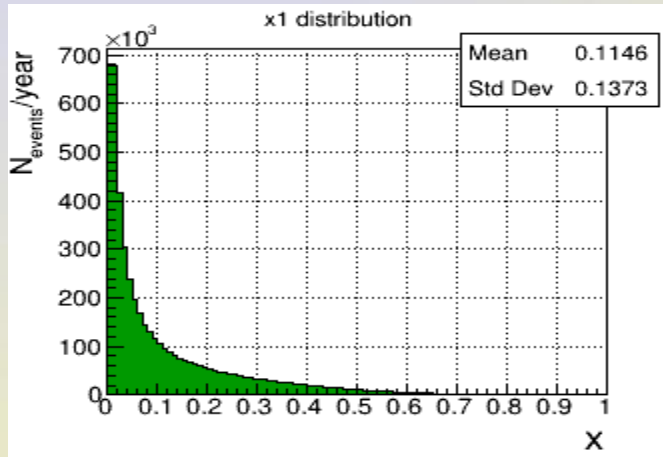
General Drell-Yan event variables for pp collision at $E_{\text{cm}} = 27 \text{ GeV}$



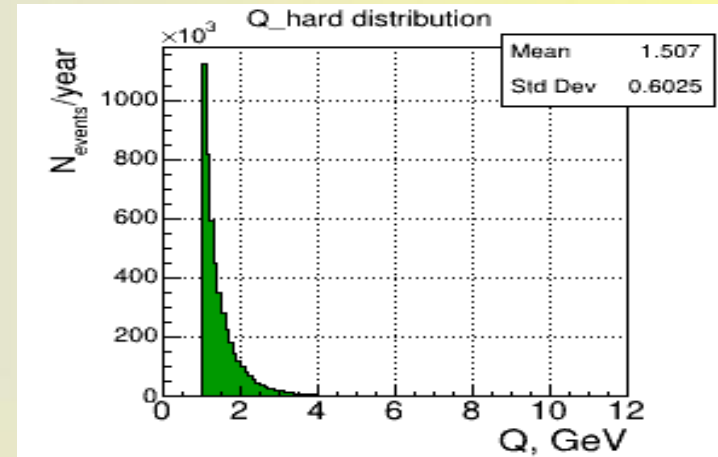
Доля импульса x , уносимая партонами

cms

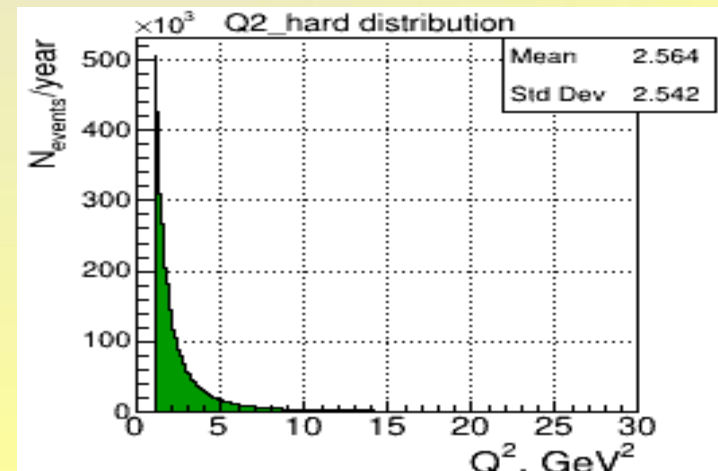
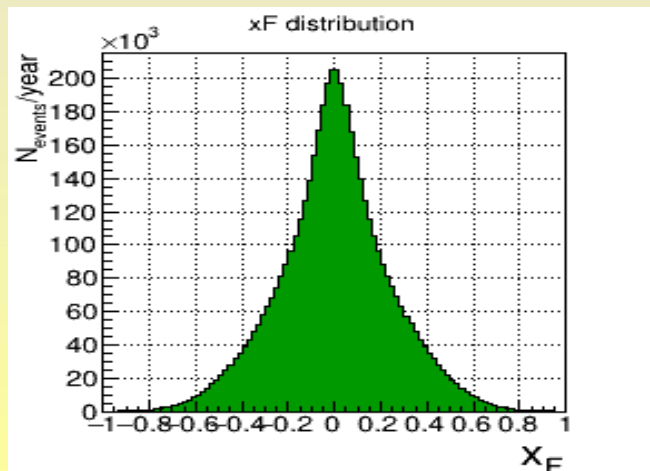
Q жесткого подпроцесса



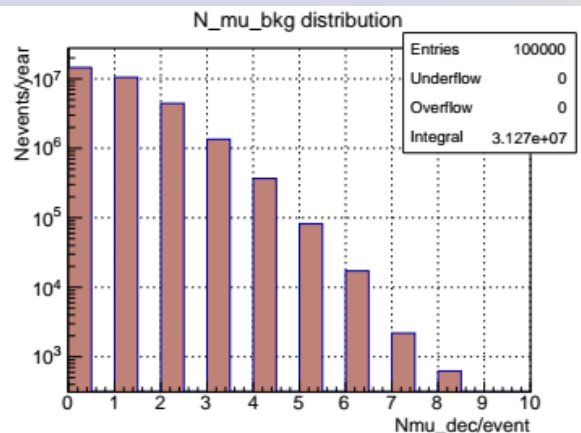
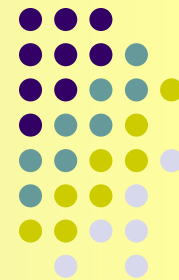
$$X = x_1 - x_2$$



Q жесткого подпроцесса

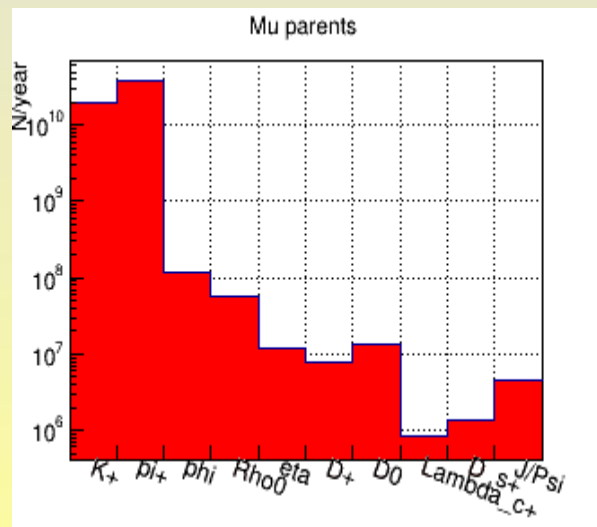


Background muons in signal events



53.5 % of signal events contains >2 muons
- up to 8 μ /event

We allow particles decay (and produce muons) in the volume before Muon (Range) System :
cylindr radius **R = 2 400 mm**,
size from the centre along Z axis **L = 4 000 mm**
and search for muons in the angle region **9° < Θ < 171°**

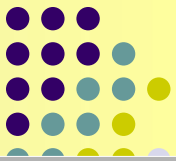


The most probable parents of bkg muons - are charged π and K

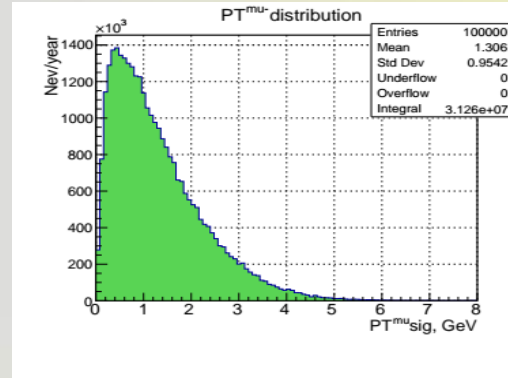
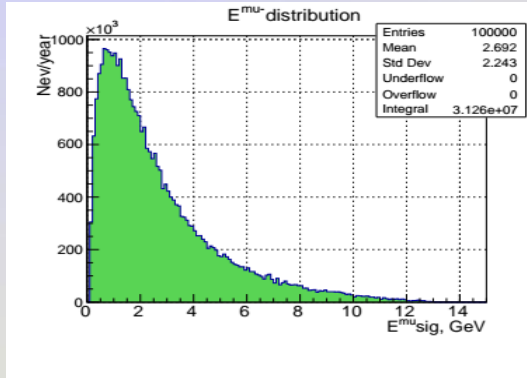
The most probable grandparents of bkg muons - are «string» (Lund model),

$$\rho^0, \rho^+, K_s^0, K_s^+, K_s^-, \eta'$$

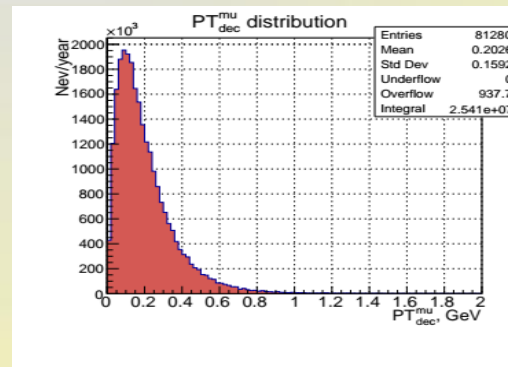
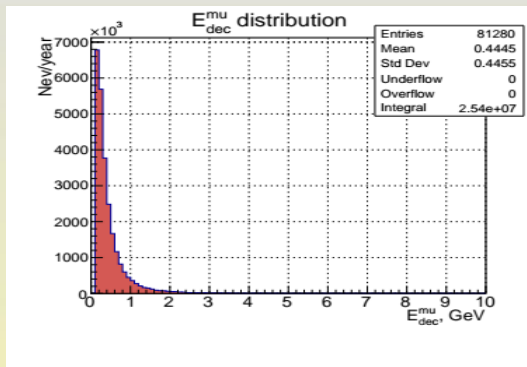
Decay muons in signal events



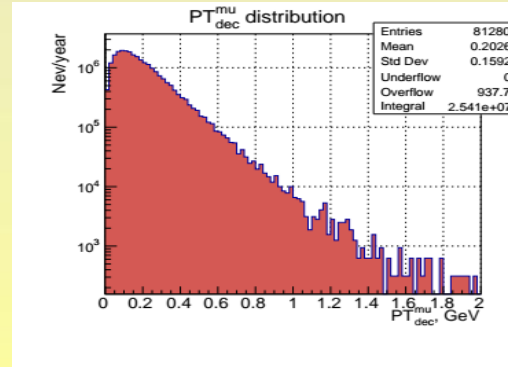
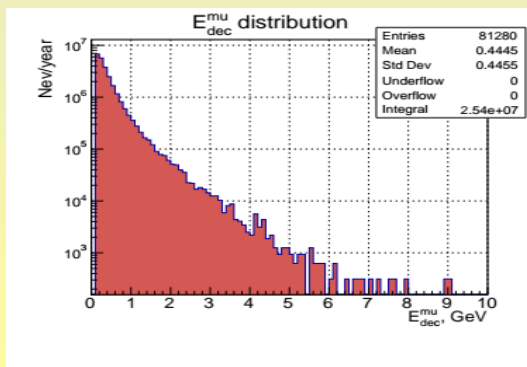
S
I
G



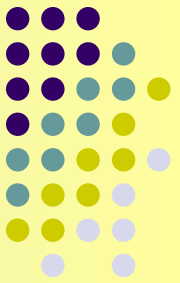
D
E
C



D
E
C
(log)



Cuts :	$E > 0.8$ GeV	$E > 1.0$ GeV
exactly 2 muons	$PT > 0.4$ GeV	$PT > 1.0$ GeV
Reminder of signal events	54.1%	23.5%
Fraction of initial signal events with additional muons	2.1%	0.08%
Fraction of remaining signal events with additional muons	3.9 %	0.3%



Another situation when we have exactly 2 μ — first signal, the second — survived fake one.

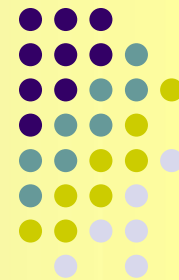
We have 2 situations -

1. Muons are of the same sign — easy to cut off
2. Muons are of different signes

After cutting off the events with additional (>2) muons we have

Cuts: exactly 2 muons with opposite signes	$E > 0.8 \text{ GeV}$ $PT > 0.4 \text{ GeV}$	$E > 1.0 \text{ GeV}$ $PT > 1.0 \text{ GeV}$
Reminder of signal events	51.9%	23.4%
Fraction of initial signal events with fake muons of the same sign	0.9%	0.09%
Fraction of remaining signal events with muons of the same sign	1.7 %	0.4%
Reminder of signal events after cut off the events with the muons of the same sign	51.0%	23.4%
Fraction of initial signal events with fake muons of different sign	0.9%	0.1%
Fraction of remaining signal events with muons of different sign	1.8 %	0.4%

Processes with charmonium production



$$\underline{1) q_i q_i^- \rightarrow \gamma^* \rightarrow c c^- \rightarrow J/\Psi \rightarrow l^+ l^- + X}$$

$$86) g g \rightarrow J/\Psi + g \rightarrow l^+ l^- + X \quad \text{R.Baier and R.Rücke, Z.Phys. C19 (1983) 251}$$

$$106) g g \rightarrow J/\Psi + \gamma \rightarrow l^+ l^- + X \quad \text{M.Drees and C.S.Kim, Z.Phys. C53 (1991) 673}$$

$$421) g g \rightarrow c c^- [^3S_1^{(1)}] g \rightarrow ll + X$$

$$422) g g \rightarrow c c^- [^3S_1^{(8)}] g \rightarrow ll + X$$

$$423) g g \rightarrow c c^- [^3S_0^{(8)}] g \rightarrow ll + X$$

$$424) g g \rightarrow c c^- [^3P_J^{(8)}] g \rightarrow ll + X$$

$$425) g q \rightarrow c c^- [^3S_1^{(8)}] q \rightarrow ll + X$$

$$426) g q \rightarrow c c^- [^3P_J^{(8)}] q \rightarrow ll + X$$

$$427) g g \rightarrow c c^- [^3S_1^{(1)}] q \rightarrow ll + X$$

$$\underline{428) q q^- \rightarrow c c^- [^3S_1^{(8)}] g \rightarrow ll + X}$$

$$\underline{429) q q^- \rightarrow c c^- [^1S_0^{(8)}] g \rightarrow ll + X}$$

$$\underline{430) q q^- \rightarrow c c^- [^3P_J^{(8)}] g \rightarrow ll + X}$$

$$431) g g \rightarrow c c^- [^3P_0^{(1)}] g \rightarrow ll + X$$

$$432) g g \rightarrow c c^- [^3P_1^{(1)}] g \rightarrow ll + X$$

$$433) g g \rightarrow c c^- [^3P_2^{(1)}] g \rightarrow ll + X$$

$$434) g q \rightarrow c c^- [^3P_0^{(1)}] q \rightarrow ll + X$$

$$435) g q \rightarrow c c^- [^3P_1^{(1)}] q \rightarrow ll + X$$

$$436) g q \rightarrow c c^- [^3P_2^{(1)}] q \rightarrow ll + X$$

$$437) q q \rightarrow c c^- [^3P_0^{(1)}] g \rightarrow ll + X$$

$$438) q q^- \rightarrow c c^- [^3P_1^{(1)}] g \rightarrow ll + X$$

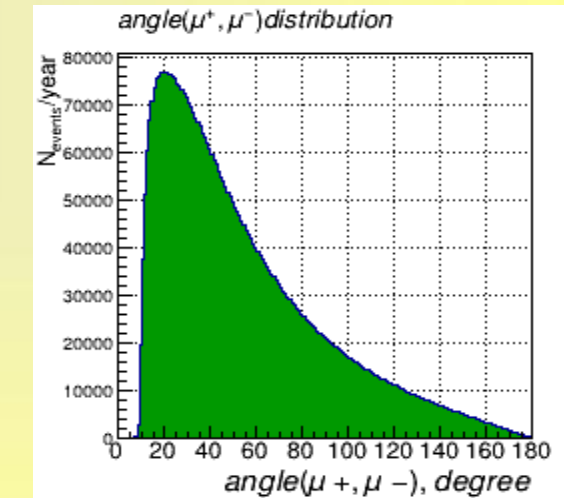
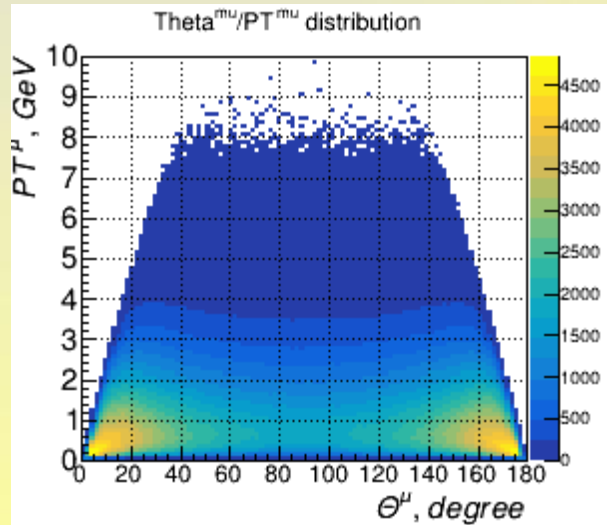
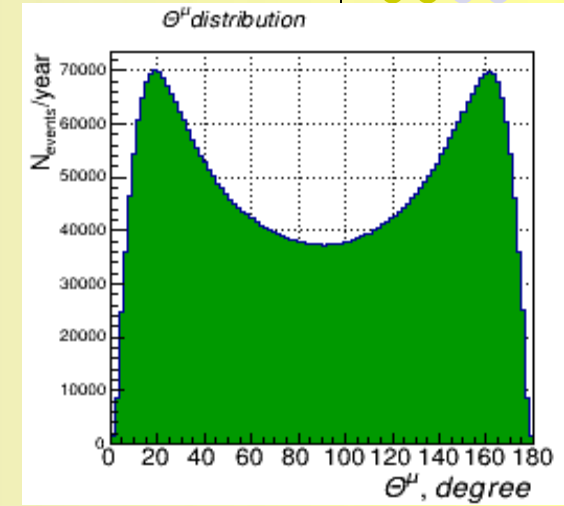
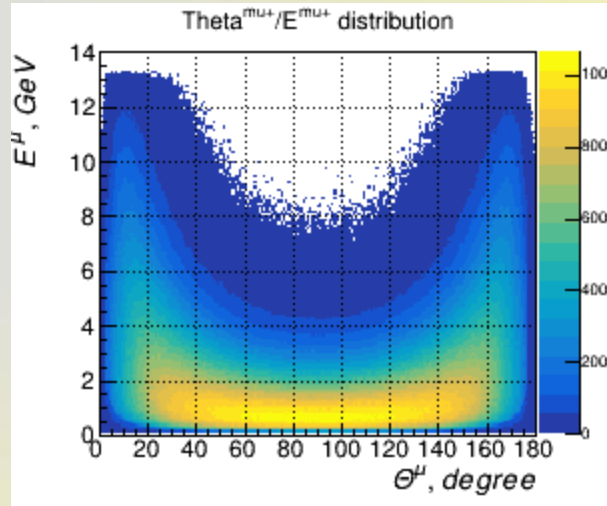
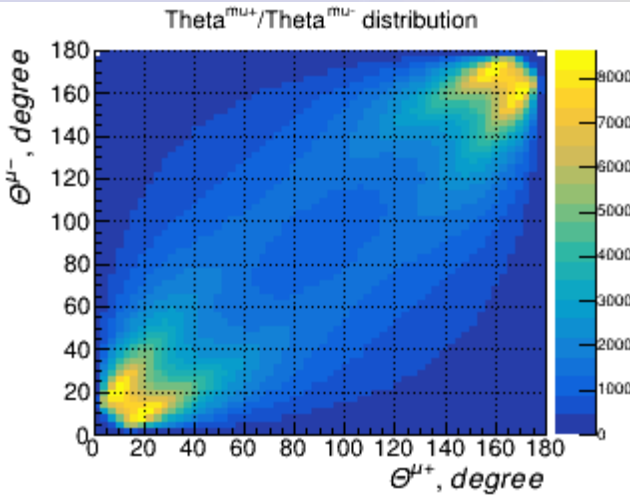
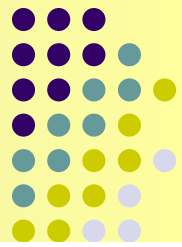
$$439) q q^- \rightarrow c c^- [^3P_2^{(1)}] g \rightarrow ll + X$$

G.T.Badwin, E.Braten and G.P.Lepage, Phys.Rev. D51 (1995) 1125 [Erratum: ibid D55 (1997) 5883];

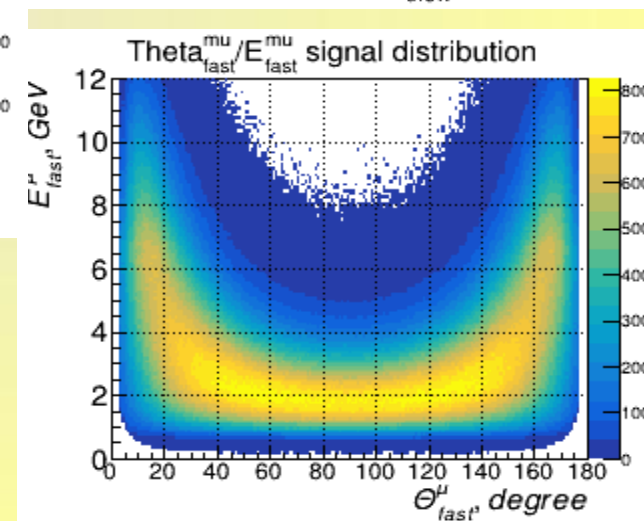
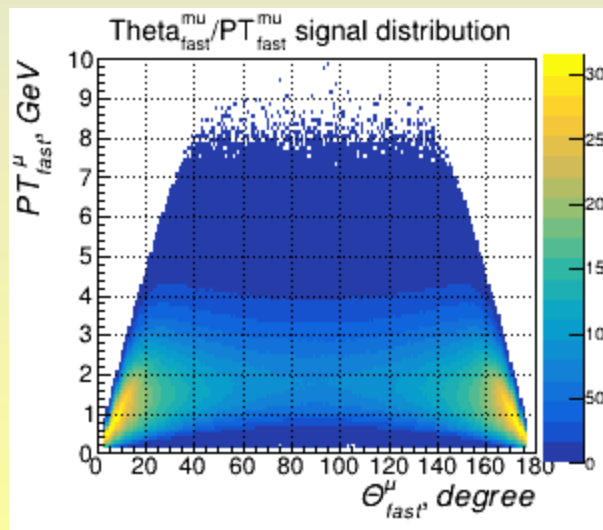
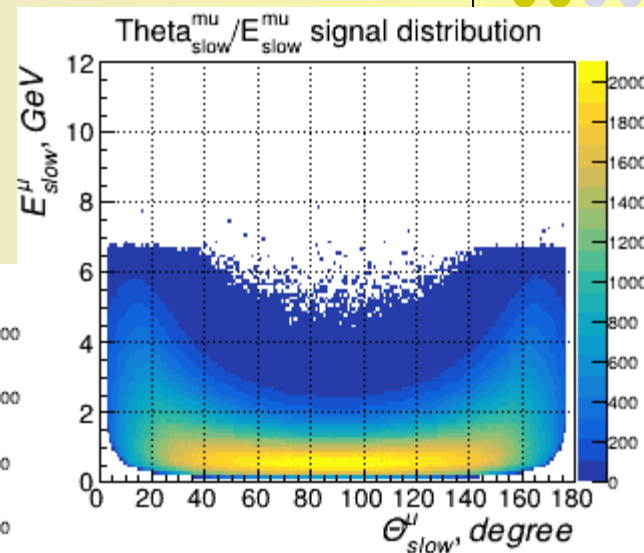
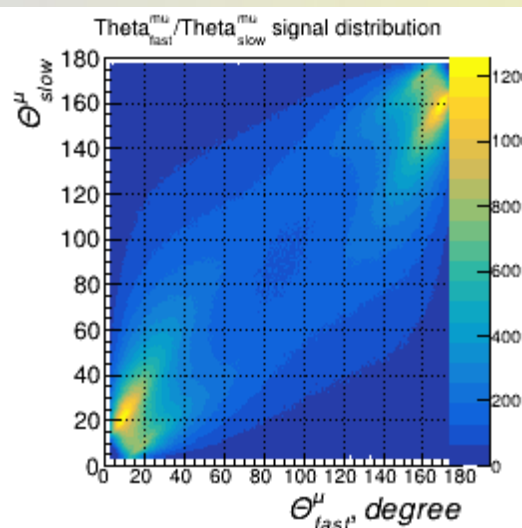
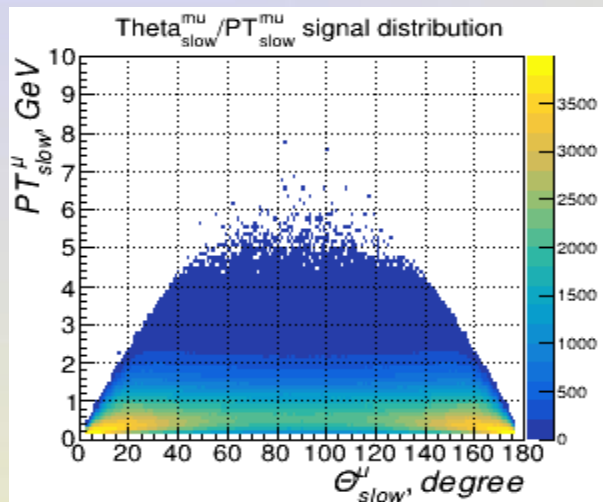
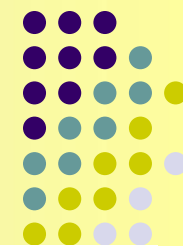
M.Beneke, M.Krämer and M.Vänttinen, Phys.Rev.D57 (1998) 4258;

B.A.Kniehl and J.Lee, Phys.Rev. D62 (2000) 114027

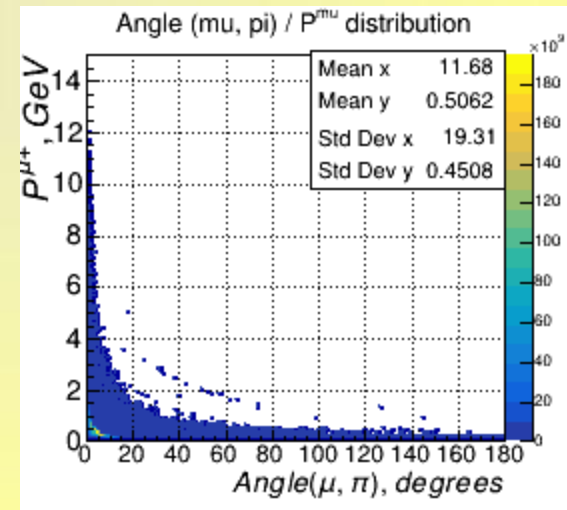
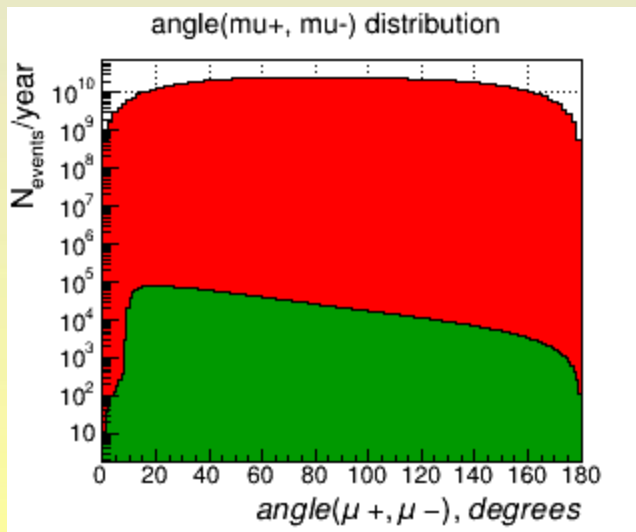
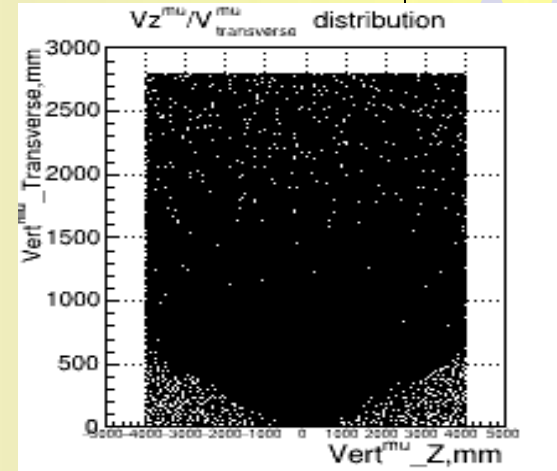
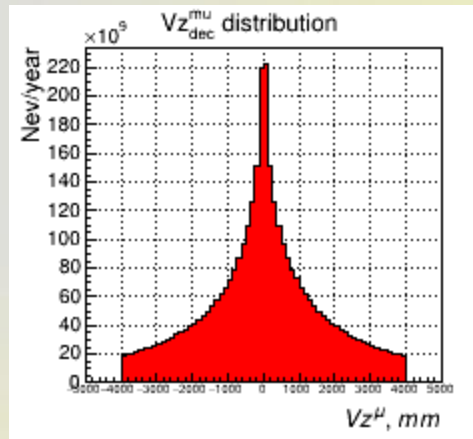
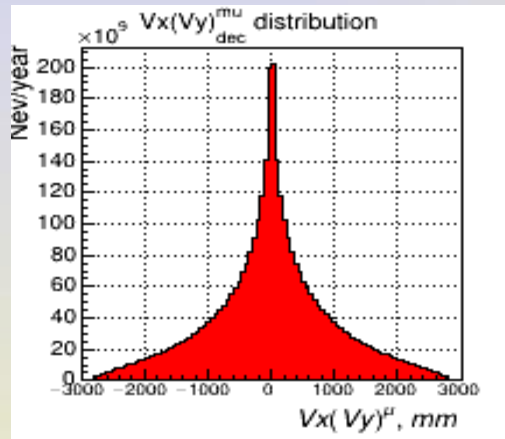
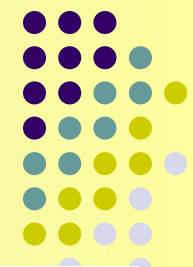
Some signal μ correlation distributions



Angle and E, PT for fast and slow signal μ correlation distributions

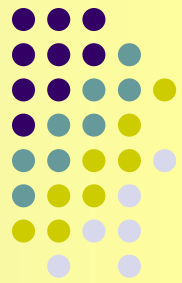


Vertex & angle distributions



P
Y
T
H
I
A

π/μ rejection



For 5λ of path length in iron.

Particle momentum	π/μ rejection
0.5 — 1 GeV	~ 80 % (experiment with MS prototype)
1 — 1.5 GeV	~ 90 % (assumption)
> 1.5 GeV	~ 99 % (assumption)

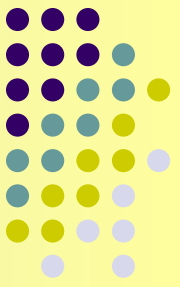
EPJ Web Conf.,
177 (2018) 04001

The path length of a charged particle track inside the sandwich structure serves as one of the most powerful variables for μ/π separation, which is challenging due to the similar rest mass of muon and pion

for 3λ path length (+4.9 % muon misidentification)
 for 4λ path length (+1.8 % muon misidentification)
 for 5λ path length (+0.67 % muon misidentification)
 $\lambda_{FE} \sim 17\text{cm}$

Cuts separate and summarized efficiency for Open Charm background events (10^7)

$$\text{Efficiency } \text{Eff}(K,N) = \text{Nev}(\text{cut}N) / \text{Nev}(\text{cut}K)$$



N of cuts	S/B ratio	Efficiency for BKG	Rest of BKG	Efficiency for SIG	Rest of SIG
1 Exactly 2μ with $PT^\mu > 0.6$ GeV, <u>$P(E)^\mu > 1.0$ GeV</u>	0.10	Eff (1,init) = 47.14	2.1 %	2.45	40.8 %
2⁺¹ 2μ are of the opposite sign	0.12	Eff (2,1) = 1.21	1.7 %	1.01	40.5 %
3⁺²⁺¹ $M_{inv}(\mu^+, \mu^-) > 1.0$ GeV	0.14	Eff (3,2) = 1.19	1.4 %	1.01	40.0 %
4⁺³⁺²⁺¹ $PT^\mu_{Emax} > 1.5$ GeV	0.82	Eff (4,3) = 8.77	1.7×10^{-1} %	1.53	26.2 %
5⁺³⁺²⁺¹ $E_{sum}^{all} > 26.8$ GeV	263.3	Eff (5,3) = 5401	2.7×10^{-4} %	2.93	13.6 %
6⁺³⁺²⁺¹ $PT_{vecsum}^{all} < 0.2$ GeV	1.18	Eff (6,3) = 14.31	1.0×10^{-1} %	1.73	23.1 %
7⁺³⁺²⁺¹ $P_{vecsum}^{all} < 0.2$ GeV	7.04	Eff (7,3) = 131.6	1.1×10^{-2} %	2.67	15.0 %
8⁺³⁺²⁺¹ Isolation criterium	> 20433	Eff (8,3) > 145845	$< 1.0 \times 10^{-5}$ %	1.02	39.3 %
9⁺³⁺²⁺¹ $R_{vertex} < 1$ mm	764.8	Eff (9,3) = 5401	2.7×10^{-4} %	1.01	39.7 %
10⁺³⁺²⁺¹ $R_{vertex} < 30$ mm	18.6	Eff (10,3) = 131.6	1.1×10^{-2} %	1.01	39.7 %
5⁺⁴⁺³⁺²⁺¹ $E_{sum}^{all} > 26.8$ GeV	1306	Eff (5,4) = 4157	4.0×10^{-5} %	2.61	10.0 %
8⁺⁴⁺³⁺²⁺¹ Isolation criterium	> 13238	Eff (8,4) > 16627	$< 1.0 \times 10^{-5}$ %	1.03	25.4 %
8⁺⁵⁺⁴⁺³⁺²⁺¹ Isolation criterium	> 5178	Eff (8,5) > 4	$< 1.0 \times 10^{-5}$ %	1.01	9.95 %